atmosphere

MDPI

Article

Employing the Method of Characteristics to Obtain the Solution of Spectral Evolution of Turbulent Kinetic Energy Density Equation in an Isotropic Flow

Charles Rogério Paveglio Szinvelski [1,*,†,‡], Lidiane Buligon [1,*,‡], Gervásio Annes Degrazia [2,‡], Tiziano Tirabassi [2,‡], Otavio Costa Acevedo [2,‡] and Débora Regina Roberti [2,‡]

1 Department of Mathematics, Federal University of Santa Maria, Santa Maria 97105900, Brazil; charless@ufsm.br (C.R.P.S.) ; buligon.l@ufsm.br (L.B.)
2 Department of Physics, Federal University of Santa Maria, Santa Maria 97105900, Brazil; gervasiodegrazia@gmail.com (G.A.D.); T.Tirabassi@isac.cnr.it (T.T.); otavio@ufsm.br (O.C.A.); debora@ufsm.br (D.R.R.)
* Correspondence: charless@ufsm.br (C.R.P.S.); buligon.l@ufsm.br (L.B.); Tel.: +55-55-9917-87138 (C.R.P.S. & L.B.)
† Current address: Federal University of Santa Maria, Santa Maria 97105900, Brazil.
‡ These authors contributed equally to this work.

Received: 30 July 2019; Accepted: 3 October 2019; Published: 10 October 2019

check for updates

Abstract: This study aims to review the physical theory and parametrizations associated to Turbulent Kinetic Energy Density Function (STKE). The bibliographic references bring a broad view of the physical problem, mathematical techniques and modeling of turbulent kinetic energy dynamics in the convective boundary layer. A simplified model based on the dynamical equation for the STKE, in an isotropic and homogeneous turbulent flow regime, is done by formulating and considering the isotropic inertial energy transfer and viscous dissipation terms. This model is described by the Cauchy Problem and solved employing the Method of Characteristics. Therefore, a discussion on Linear First Order Partial Differential Equation, its existence, and uniqueness of solution has been presented. The spectral function solution obtained from its associated characteristic curves and initial condition (Method of Characteristics) reproduces the main features of a modeled physical system. In addition, this modeling allows us to obtain the scaling parameters, which are frequently employed in parameterizations for turbulent dispersion.

Keywords: atmospheric turbulence; models parameterizations; characteristic curves; method of characteristics; first order PDE(s); isotropy; three-dimensional spectrum of turbulent kinetic energy; dynamic equation of spectral function

---

1. Introduction

The model that describes the dynamics of Turbulent Kinetic Energy (TKE) under the hypothesis of regime fully developed turbulence covers several arguments associated with the phenomenology of the physical system [1]. Due to the complexity of the phenomenon, an idealized representation based on parametrizations is necessary, therefore, the accuracy of the model formulated depends on the ability of the constituent equations to mathematically describe the physical process.

In this sense, the spectral energy density dynamics model in the Convective Boundary Layer (CBL) is based on a system of Partial Differential Equations (PDE) known as Navier-Stokes Equations [1], in which the predicted TKE evolution in the CBL is admitted from the parameterization of the forms of production, dissipation, and energy transfer.

To define these basic descriptive terms of the spectral dynamics, it is necessary to establish the object of study itself, which is the Spectral Density Turbulent Kinetic Energy Function (STKE), and subsequent quantification as TKE of the CBL as a manifestation of the turbulent flow velocity fluctuations. For this, we must begin with the conception of the autocorrelation functions and 1D spectral density function by the Fourier transform [2], until its representation in the three-dimensional form [3] and later synthesis in a descriptive equation of the dynamic spectral function [1].

At this point, the importance of the parameterization process of the constituent terms of the model is emphasized, as it will not only indicate the reliability of the model through the realistic description of the involved processes and reproduction of observed properties in the phenomenon, but also influence the choice of mathematical methods (analytical and/or numerical) to obtain the solution [4].

In this manuscript, the parameterizations for the terms of production, dissipation and energy transfer are presented [5]. However, as it is considered a simplified model that only involves the inertial transfer of TKE and dissipation terms describe these dynamics, this assumption allows us to obtain a model composed of a Linear First Order Partial Differential Equation (1L-PDE), which can be solved using the Method of Characteristics [6,7].

The choice of this method will be evidenced by not being a restrictive method, that is, it applies to any first order PDE (1st-PDE) and allows the use of numerical techniques that are easily incorporated by the method [4,8]. Moreover, it allows an understanding of the process of developing the solution, which indicates the steps for a demonstration of the Theorem of Existence and Uniqueness of solutions for 1L-PDE.

At the end, this paper presents a modeling process of a natural phenomenon, starting from the specification and characterization of the object of study, its genesis, parameterization of related processes, construction of an idealized equation of modeling of the phenomenon, and later detailing and theoretical demonstration of validity and applicability of the method to obtain the solution. Then, the solution obtained in this simplified model will reproduce the basic properties of the modeled dynamics.

The study is composed of two essential sections to comprehend the proposed modeling process. The first section covers the theoretical framework that aims to describe the relevant physical processes associated to the phenomenon of turbulence that will be employed in the formulation of a Spectral Density Evolution Equation of TKE in a CBL. It starts from the conception of the pair of functions of autocorrelation and one-dimensional energy density via Fourier transform and the elaboration of its three-dimensional spatial variation. Once the STKE is established, an equation taken from [1] will relate the temporal evolution of the STKE dynamics together with terms of production, dissipation, and STKE transfer in CBL. To better understand the processes involved in this dynamic model, the parameterizations of these terms are described. It is worth noting that these parametrizations present non-stationary elements inherent to the turbulent flow, such as convective boundary-layer height (z_i), friction velocity (u^*), Obukhov length (L), convective velocity scale (w^*), among others [9]. These scaling parameters are used to make the proposed equations dimensionless and, enable us to describe the models of the general time, length, and velocity scales parameters [5]. The second section consists of questions associated with the Method of Characteristics, which is the respective mathematical method employed to obtain the solution of the presented physical model. A two-stage presentation of the method in question was chosen. In the first stage, the generalized geometric construction of the solution surface itself is given, and as a complementary section to this geometric description, Appendix A outlines a general idea of the method application, processes, and geometric entities involved in constructing the solution surface by solving a simplified 1st-PDE. In the second stage, the mathematical proof that validates the solution surface constructed as a solution of the 1L-PDE is established. Once the procedures and techniques of the theoretical foundation are established, a generic model for STKE in the CBL can be formulated. Finally, the Isotropic Model for the STKE dynamics in the PBL is established. This model is designed by simplifying isotropic turbulence hypotheses and non-STKE production by thermal and mechanical convection and its solution is obtained by the Method of Characteristics.

2. Theoretical Framework

The theoretical framework applied in the formulation of the 3D-STKE and relevant processes that describe the dynamics of the TKE in the CBL are presented here. The mathematical hypothesis to solve a 1L-PDE by the Method of Characteristics will be made through a geometric approach to develop this solution by the characteristic curves with the PDE and afterwards extend the process to general 1L-PDE [6,7,10].

2.1. The Turbulent Energy Spectrum Function

Assuming that particle movement can be determined by velocity fluctuations in a turbulent flow and quantification of this buoyancy is given by Autocorrelation Function

$$\left\langle u^2 \right\rangle R(\tau) = \langle u(t)u(t+\tau)\rangle . \tag{1}$$

This generic Autocorrelation Function, with the property of $R(0) = 1$, indicating that the maximum correlation in the measurement of the wind velocity buoyancy occurs for $\tau = 0$ and to others values of τ $|R(\tau)| \leq 1$ [11], being a quantifier of the ability of the particle to preserve the memory of the effect of a given velocity at a given instant in the composition of the velocity of this particle later [2].

Reference [12] establishes a statistical theory for treating and modeling these turbulent flows under the hypotheses of isotropy, homogeneity, and stationarity of turbulence (Taylor's Turbulent Diffusion Theory) and proposes an exponential form for the autocorrelation function and obtained fundamental relations related to the study of the phenomenon of turbulence applied to scalar dispersion [13].

In this aspect, autocorrelation functions in the Taylor Statistical Theory [12] allow us to calculate the dispersion parameters and functional relations for the turbulence dissipation rate used in Eulerian and Lagrangian dispersion models [9,11,14–17], which leads to the opening of a vast field of research in the area of turbulence modeling in its various phenomenological manifestations. These studies address issues related to developing new autocorrelation functions and functions associated with turbulent parameter deductions [18–20] and validation [1,11,21,22].

Among these results, the Wiener Khintchin theorem [23] relates the autocorrelation function $R(\tau)$ with the spectral function $\Phi(\omega)$ via the Fourier transform pair:

$$R(\tau) = \frac{1}{\langle u^2 \rangle} \int_{-\infty}^{+\infty} \Phi(\omega) e^{-i\omega\tau} d\omega \quad \text{and} \quad \Phi(\omega) = \frac{\langle u^2 \rangle}{2\pi} \int_{-\infty}^{+\infty} R(\tau) e^{i\omega\tau} d\tau, \tag{2}$$

where ω is the turbulent frequency and $\langle u^2 \rangle$ is the turbulence velocity variance.

Under the assumption of stationary and homogeneous turbulence and $R(\tau)$ being a pair function and $\tau = 0$, the relation obtained is:

$$\frac{1}{2} \langle u^2 \rangle = \int_{0}^{+\infty} \Phi(\omega) d\omega, \tag{3}$$

evidenced that the TKE is the result of the integration over the entire frequency range of the STKE. This is consistent with the hypothesis proposed, since quantifying the buoyancy via the turbulent velocity variance enables the extraction of auxiliary information to determine typical speed and length scales to obtain the parameters applied to describe of turbulent flows [24].

The pair of equations given by Equation (2) states that STKE is obtained by the Fourier transform of the autocorrelation function. As shown above, this tool amplifies the understanding of the processes of analyzing turbulent energy dynamics through the frequency and/or wave number decomposition of functions used to describe these STKE dynamics [2]. This description allows the visualization of the processes of these dynamics through the exchange of energy between the eddies of different sizes of wave number or frequency. A description of the typical regions of occurrence of these processes is described in Figure 1.

The idea of a turbulent flux composed of interagency eddies on the various scales of size and frequency suggests that the process is random in the three spatial directions and in time, as emphasized by [2], characterizing turbulence as a three-dimensional phenomenon. In this sense, experiments for its measurement, in addition to the financial cost, have inherent technical challenges. Experimental STKE measurements are one-dimensional in their respective spatial directions and in time [25], with a three-dimensional STKE being determined from one-dimensional measurements [3,26,27]. If these measurements are obtained in stationarity situations, the autocorrelation function is defined over time $(t\,[u.t.])$ and, consequently, the STKE will be in the frequency domain $\omega\,[u.t.]^{-1}$. If it is in conditions of homogeneous turbulence, the autocorrelation function will be given in the spatial variables $(x_i,\ i = 1,2,3.\,[u.c.])$ and its Fourier transform in the wave number domain $k_i,\ i = 1,2,3\,[u.c.]^{-1}$ [2].

Notably, one-dimensional spectra do not include the full information of the three-dimensional turbulence phenomenon in CBL, and for certain ranges of wave number values, the spectrum measured in a particular direction may contain vortex contributions, that when aligned to this direction of measurement, if wave numbers are higher than those of the specified range, msy charactere the *aliasing* phenomenon [2].

The previous paragraphs suggest that we use a spatial autocorrelation function defined in $\mathbf{x} = (x_1, x_2, x_3)$ to better representat the three-dimensional turbulent flow and avoid the aliasing phenomenon, consequently resulting in the STKE to occur in the wave number vector $\mathbf{k} = (k_1, k_2, k_3)$ by the three-dimensional Fourier transform ([28] (p. 161) and [1].)

However, in order to overcome the difficulty of adding directional information, it is necessary to consider a spherical envelope around a reference point, which is the origin of this envelope. Fixed at the origin, it is assumed that $\mathbf{U} = \langle \mathbf{u}(\mathbf{x}) \rangle$ - preferential average velocity (a preferred and constant mean velocity is assumed for the three-dimensional field of velocities $\mathbf{u} = (u_1, u_2, u_3) = (u, v, w)$, where u is the longitudinal wind velocity, v is the lateral wind velocity, and w is the vertical wind velocity) is constant and along this constant direction aligns the directional $\mathbf{i}_1 = \hat{\mathbf{i}}$. The vertical direction is naturally fixed ($\mathbf{i}_3 = \hat{\mathbf{k}}$) and the lateral direction is then defined by vector product $\mathbf{i}_1 \times \mathbf{i}_3 = \mathbf{i}_2 = \hat{\mathbf{j}}$. In this new configuration of the space and consequent reconfiguration of the space of the wave number vector, the magnitude of the wave number vector is given by $k = \sqrt{\mathbf{k} \cdot \mathbf{k}} = ||\mathbf{k}||$, which is the radius of this spherical envelope. When integrating this spherical envelope, the total energy over k—the three-dimensional energy spectrum is obtained [2,3].

Although the association of the spatial autocorrelation function and its STKE via Fourier transform has already been referenced, it is necessary to establish certain conditions in turbulent flow to perform this association.

In the first stage, the isotropy condition will not be required for the turbulent flow, although homogeneity will be admitted to the wind field, as well as stationarity—the effects of turbulent flow on the wind component measurement is invariant on translations. Under these hypotheses and by employing Reynold decomposition to wind components given by $\mathbf{u}(\mathbf{x}) = \mathbf{U}(\mathbf{x}) + \mathbf{u}'(\mathbf{x}) \Leftrightarrow u_i = U_i + u_i',\ i = 1,2,3$, the Correlation Tensor can be associated with the turbulent moments: $\mathbf{R}_{ij}(\mathbf{r}) = \langle u_i'(\mathbf{x}) u_j'(\mathbf{x} + \mathbf{r}) \rangle$

$$\mathbf{R}_{ij}(\mathbf{r}) = \big\langle \left(u_i(\mathbf{x}) - \mathbf{U}\right)\left(u_j(\mathbf{x} + \mathbf{r}) - \mathbf{U}\right) \big\rangle .$$

The Correlation Tensor is said to be symmetrical and invariant due to reflections and translations $\left(\mathbf{R}_{ij}\left(-\mathbf{r}\right)=\mathbf{R}_{ji}\left(\mathbf{r}\right)=\mathbf{R}_{ij}\left(\mathbf{r}\right)\right)$ and thus impose the STKE Tensor as the Fourier transform of the Correlation Tensor [2,3]:

$$\mathbf{\Phi}_{ij}\left(\mathbf{k}\right)=\frac{1}{(2\pi)^3}\int_{-\infty}^{\infty}\int_{-\infty}^{\infty}\int_{-\infty}^{\infty}\mathbf{R}_{ij}\left(\mathbf{r}\right)\exp\left(-i\mathbf{k}\cdot\mathbf{r}\right)d^3r\ \ (d^3r=dr_1\,dr_2\,dr_3) \tag{4}$$

and its transformed pair

$$\mathbf{R}_{ij}\left(\mathbf{r}\right)=\int_{-\infty}^{\infty}\int_{-\infty}^{\infty}\int_{-\infty}^{\infty}\mathbf{\Phi}_{ij}\left(\mathbf{k}\right)\exp\left(i\mathbf{k}\cdot\mathbf{r}\right)d^3k\ (d^3k=dk_1\,dk_2\,dk_3). \tag{5}$$

The tensor $\mathbf{\Phi}_{ij}$ is symmetric, which is a result of the velocity field homogeneity, characterizing it as a covariant tensor in space-k. Moreover, the property of atmospheric incompressibility is valid ([3] *apud* [29]) and equivalent to

$$\sum_j \mathbf{\Phi}_{ij}(\mathbf{k})k_j=0. \tag{6}$$

Equation (6) characterizes $\mathbf{\Phi}_{ij}$ as a semidefinite positive tensor, that is, there are no negative eigenvalues associated with the eigenvectors $\mathbf{k}$, ensuring $\mathbf{\Phi}_{ij}$ to be a genuine covariant tensor [3].

The sum of main diagonal of the STKE tensor $\left(\sum\mathbf{\Phi}_{ii}\right)$ is associated to

$$\int_{-\infty}^{\infty}\int_{-\infty}^{\infty}\int_{-\infty}^{\infty}\sum\mathbf{\Phi}_{ii}\left(\mathbf{k}\right)d\mathbf{k}=\sum\langle u_i'u_i'\rangle\ \left(=\sum\mathbf{R}_{ii}(\mathbf{0})\right).$$

Directional information ii is removed in the integration process in the spherical envelope of radius k with surface element $d\sigma$ [2,3,30]. Defining

$$\mathbf{E}(k)=\frac{1}{2}\oiint_S\sum\mathbf{\Phi}_{ii}(\mathbf{k})d\sigma=\frac{1}{2}\int_0^{2\pi}\int_0^{\pi}\sum\mathbf{\Phi}_{ii}k^2\sin\phi d\theta d\phi, \tag{7}$$

consequently, the total energy will be obtained under the integration of all wave numbers k [2,30] and by Equation (7):

$$E_T=\int_0^{+\infty}\mathbf{E}(k)dk=\frac{1}{2}\int_0^{+\infty}\left(\oiint_S\sum\mathbf{\Phi}_{ii}(\mathbf{k})d\sigma\right)dk=\frac{1}{2}\int_{-\infty}^{\infty}\int_{-\infty}^{\infty}\int_{-\infty}^{\infty}\sum\mathbf{\Phi}_{ii}\left(\mathbf{k}\right)d\mathbf{k}=\frac{1}{2}\sum\langle u_i'u_i'\rangle. \tag{8}$$

Maintaining the one-dimensional premise (Equation (3)) for the three-dimensional case.

Under the hypothesis of fully developed turbulence, typical characterizations of the properties and processes that compose the three-dimensional turbulent energy spectrum according to the magnitude of the wave number vector k are shown in Figure 1. The following is a brief description of these characteristics:

- The first region corresponds to the low number of waves (low-frequency) is divided into two parts. In general, the range that starts close to zero to k_1 does not contain most of the total turbulent energy. However, this is where the entrance of energy through mechanical sources occurs (denoted **M**) by the mean wind shear and thermal sources (denoted **H**), which produce thermal instability. In it, eddies are anisotropic and their properties depend on how they were generated. In addition, the largest eddies interact with the contours and layer of inversion of Planetary Boundary Layer (PBL) in this region. Nevertheless, the presence of the most energetic eddies is verified by the interval (k_1,k_2) and, thus, these eddies contain the largest portion of the total TKE;
- The second region is called the inertial subinterval and corresponds to the range of the wave numbers k_2 to k_3, being the turbulence isotropic or close to the isotropic condition. In this interval

energy, it is neither generated nor consumed, it is only transferred from large to small eddies at a rate ϵ per unit mass. This highlights the performance of a TKE transfer mechanism, noted by **W**, in the turbulent flow. The turbulence in this interval is stationary and entirely determined by rate ϵ [31], terefore one can apply the $(-5/3)$ law of Kolmogorov to describe the STKE $(\mathbf{E}\,(k))$ in this range and given by:

$$\mathbf{E}\,(k) = \alpha\epsilon^{2/3}k^{-5/3}\;(\alpha\;-\;\text{Kolmogorov constant}).$$

- The third region corresponds to high wave numbers (high-frequency), where the viscous forces of molecular origin dissipate TKE in the form of heat.

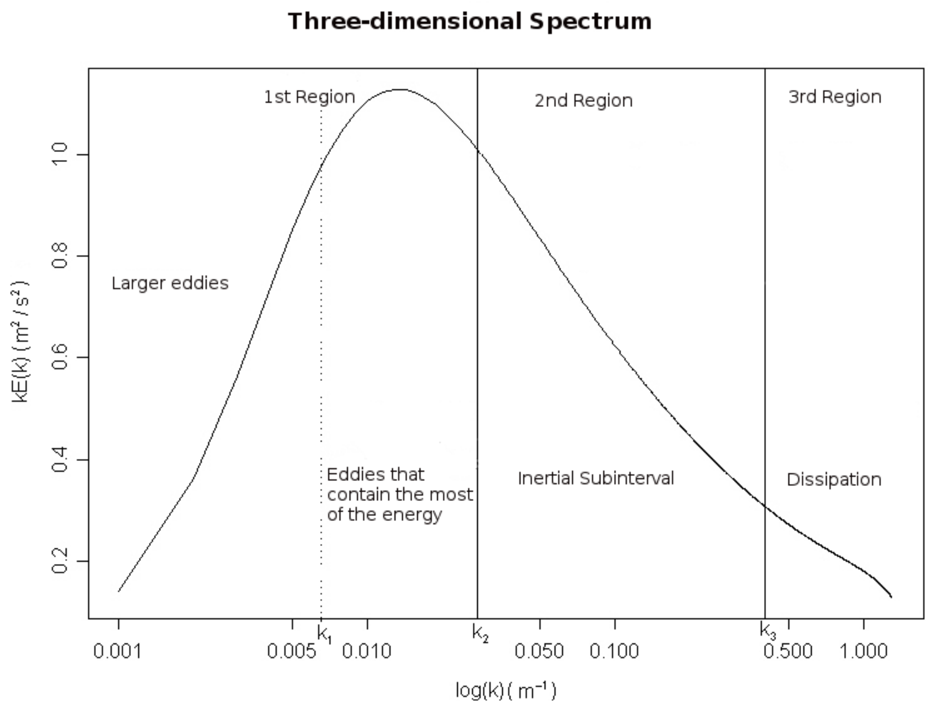

Figure 1. Three-dimensional energy spectrum for fully developed turbulence. Source: Figure adapted from [32].

2.2. Model Evolution for the STKE in CBL

A reproduction of the deduced dynamic equation of the three-dimensional Energy Spectrum (3D-STKE) demonstrated in [1] (see also [33]), which is presented in [4,5]. The dynamical equation is

$$\frac{\partial}{\partial t}\mathbf{E}\,(k,t) = \mathbf{H}\,(k,t)\,\frac{g}{\Theta_0} + \mathbf{M}\,(k,t) + \mathbf{W}\,(k,t) - 2\nu k^2\mathbf{E}\,(k,t)\,. \tag{9}$$

The terms that compose this equation relate the temporal variation of the energy spectrum function (lhs term) with the term of production or consumption of thermal convection of TKE (first term in rhs), the production of energy by mechanical effect (second term), and the inertial transfer of kinetic energy, which occurs in the direction of the largest eddies to the smallest ones characterizing the cascade effect (third term), and energy dissipation by molecular viscosity (fourth term), respectively.

Assuming that Equation (9) governs the temporal evolution of the STKE, a model will develop as the description of the constitutive equations of this equation is made. After these parameters are formed plus the insertion of an initial condition (IC), an Initial Value Problem (IVP) is obtained and, consequently, it is possible to elaborate a model that aims to describe such evolution.

The parametrization of these constitutive equations will be related to the characteristics of the turbulent flow and examples of parametrizations can be found in [4,5,34–37]. More specifically, for models that describe CBL growth, ref. [8,37,38] show specific parametrizations of these terms. For STKE decay in CBL, ref. [5,39] can be cited.

Equation (9) is the idealized basis of a model that aims to predict TKE evolution in CBL. However, the establishment of the model will occur by parameterizing the constituent terms of this equation, which is where the most sensitive passage of its elaboration lies.

At first, elaborating these parameters agglutinates information and relationships involved in the events that constitute the phenomenon and, the more realistic this parameterization, the more reliability will be added to the model. Additionally, techniques and methods used to obtain the solutions of this model are intrinsically linked to the expressions and mathematical operations used to describe these parameters.

Due to the importance of understanding the model and its respective resolution, the parameterizations of the constituent terms of Equation (9) with their respective descriptions and dimensionless parameters and variables are displayed.

To non-stationarity of CBL, the delimiting parameters such as height, length scales, and typical velocities that describe it are variable in time and space. A dimensionless process is done by considering the set of generalized terms to describe the variability of terms such as convective boundary layer, convective velocity, ... :

$$t_* = \frac{w_* t}{z_i},\ R_e = \frac{w_* z_i}{\nu},\ \psi_\epsilon = \frac{\epsilon z_i}{w_*^3},\ k' = kz_i \text{ and } S(z) = \frac{\phi_m u_*}{\kappa z},$$

where w_* is the characteristic convective velocity scale $[m/s]$, z_i the height of the CBL $[m]$, Re is the Reynolds number (ν the molecular viscosity coefficient $[m^2/s]$), ψ_ϵ is the dimensionless thermal dissipation rate, ϵ the mean thermal dissipation rate of TKE $[m^2/s^3]$, u_* the wind shear velocity $[m/s]$, ϕ_m the dimensionless mechanical dissipation rate, $S(z)$ the variation in z of the mean velocity $[s^{-1}]$, and κ the von Kármám constant [5].

2.2.1. Thermal Convection

In Equation (9), the term $\frac{g}{\Theta_0}\mathbf{H}(k,t)$ is responsible for describing the production loss of kinetic energy by thermal convection. It will be decomposed into the product between a term that depends only on the wave number and another term that only depends on time [4,5], that is,

$$\frac{g}{\Theta_0}\mathbf{H}(k,t) = \frac{g}{\Theta_0} H_0(k) T(t), \tag{10}$$

where $T(t)$ is a function that describes the temporal growth of surface heat flux and $H_0(k)$ that only depends on the characteristic conditions of the CBL in a fully developed turbulence regime.

The hypothesis of [14] will be considered to determine $H_0(k)$, which assumes that the energy transfer from the mean flow to the turbulent flow occurs continuously. Such analysis does not consider any time scale characteristic of the parameterization. Assuming that $H_0(k)$ depends on the potential temperature gradient $\left(\frac{\partial\theta}{\partial z}\right.$, where in the well mixed layer, it will be replaced by the term of countergradient γ_c, since to the process of entrainment of the upper part of the CBL, there is heat flowing from cold to hot regardless of the local gradient of the background environment, which contains large eddies associated with the rise of warm air parcels that transport heat from hot to cold $\left.[33]\right)$, the wave number k, kinetic energy dissipation ratio ϵ_0, and kinetic energy intensity centered around the number of wave k, that is, $k\mathbf{E}_0(k)$, where $\mathbf{E}_0(k)$ is the three-dimensional spectral density of the well-developed convective boundary layer, the following result can written through a dimensional analysis:

$$\frac{g}{\Theta_0} H_0(k) = \frac{g}{\Theta_0} \gamma_c c_1 \epsilon^{-1/3} k^{-2/3} \mathbf{E}_0(k) \tag{11}$$

where c_1 is a constant to be determined from the initial conditions [4]—Appendix A.

Using the definition of convective velocity, one obtains:

$$\frac{g}{\Theta_0} = \frac{w_*^3}{z_i} \overline{(w\theta)_0} \tag{12}$$

where $\overline{(w\theta)_0}$ is the surface heat flux, w_* is the convective velocity, and z_i is the height of the CBL [33].

For function $T(t)$, which describes the growth in time of $\mathbf{H}\,(k,t)$, the equation suggested by [40] is written as:

$$T(t) = \sin(\Omega t), \tag{13}$$

where Ω is the angular frequency.

By substituting Equations (11)–(13) for Equation (10), the following formulation for the production or loss term of energy due to thermal buoyancy is obtained [4,5,39,41]:

$$\frac{g}{\Theta_0} \mathbf{H}\,(k,t) = \frac{w_*^3}{z_i} \overline{(w\theta)_0} \gamma_c c_1 \epsilon^{-1/3} k^{-2/3} \mathbf{E}_0(k) \sin(\Omega t).$$

The dimensionless form is given by:

$$\begin{aligned}
\frac{g}{\Theta_0} \mathbf{H}\,(k,t) &= \frac{g}{\Theta_0} H_0(k) T(t) = \left(\frac{g}{\Theta_0} \gamma_c \frac{c_1 \mathbf{E}_0(k)}{\epsilon^{1/3} k^{2/3}} \right) \cdot \sin(\Omega t) = \left(\frac{w_*^3 \frac{\partial\theta}{\partial z}}{\left(\bar{w\theta}\right)_0 z_i} \frac{c_1 \mathbf{E}_0(k)}{\epsilon^{1/3} k^{2/3}} \cdot \frac{z_i^{2/3}}{z_i^{2/3}} \frac{w_*}{w_*} \right) \cdot \sin\left(t_* \frac{z_i \Omega}{w_*} \right) \\
&= \left(\frac{w_*^3 \frac{\partial\theta}{\partial z}}{\left(\bar{w\theta}\right)_0} \frac{c_1 \mathbf{E}_0(k)}{(k z_i)^{2/3}} \frac{w_*}{\epsilon^{1/3}} \frac{z_i^{2/3}}{z_i w_*} \right) \cdot \sin\left(\frac{z_i \Omega}{w_*} t_* \right) = \left(\frac{w_*^2 \frac{\partial\theta}{\partial z}}{\left(\bar{w\theta}\right)_0} c_1 (k')^{-2/3} \frac{w_* \mathbf{E}_0(k')}{(z_i \epsilon)^{1/3}} \right) \cdot \sin\left(\frac{z_i \Omega}{w_*} t_* \right) \\
&= \left(\frac{w_*^2 \frac{\partial\theta}{\partial z}}{\left(\bar{w\theta}\right)_0} \frac{c_1 \mathbf{E}_0(k')}{\psi_\epsilon^{1/3} (k')^{2/3}} \right) \cdot \sin\left(\frac{z_i \Omega}{w_*} t_* \right) = \left[\frac{w_* z_i}{\left(\bar{w\theta}\right)_0} \frac{\partial\theta}{\partial z} c_1 \psi_\epsilon^{-1/3} (k')^{-2/3} \mathbf{E}_0(k') \sin\left(\frac{z_i \Omega}{w_*} t_* \right) \right] \frac{w_*}{z_i} \\
&= \left[H_0(k') T(t_*) \right] \frac{w_*}{z_i} = \mathbf{H}\,(k', t_*) \frac{w_*}{z_i}.
\end{aligned} \tag{14}$$

The relationship between $\mathbf{E}_0(k)$ and Equation $\mathbf{E}_0(k')$ is made considering the isotropic limit condition of the construction process of a simplified spectral model of anisotropic turbulence presented in [3]. This model assumes that is possible to specify completely $\boldsymbol{\Phi}_{ij}(\mathbf{k})$ from the one-dimensional spectrum at one point. Under hypothesis of homogeneous turbulence in all directions [3], the initial spectrum $\mathbf{E}_0$ can be obtained from anisotropic turbulence condition, which has isotropic turbulence condition (Equation (15)) as limit case . The dimensionless initial spectrum is given by

$$\mathbf{E}_0(k) = k^3 \frac{d}{dk} \left(\frac{1}{k} \frac{dF_u}{dk} \right) = \left[k^3 \frac{d}{dk} \left(\frac{1}{k} \frac{dF_u}{dk} \right) \right] \frac{z_i^3}{z_i^3} = (k')^3 \frac{d}{dk'} \left(\frac{1}{k'} \frac{dF_u}{dk'} \right) = \mathbf{E}_0(k'). \tag{15}$$

where F_u is the longitudinal one-dimensional spectrum.

2.2.2. Mechanical Energy Production

The term $\mathbf{M}\,(k,t)$ describes the turbulence resulting from the interaction of the turbulent momentum flux with a situation of average wind shear. Since the largest magnitudes of this shear occur near the surface, there is significant contribution of turbulence due to shearing in this region [33].

In a process of dimensional analysis (see [2] for the definition of this theoretical tool of turbulence analysis) [36] (*apud* [42]) suggest the following parameterization for the mechanical energy production term:

$$\mathbf{M}\,(k,t) = c_m S(z) \epsilon^{-\frac{1}{3}} k^{-\frac{2}{3}} \mathbf{E}\,(k,t)\,,$$

and its dimensionless form:

$$\begin{aligned}\mathbf{M}(k,t) &= c_m S(z)\epsilon^{-\frac{1}{3}}k^{-\frac{2}{3}}\mathbf{E}(k,t)\times\frac{z_i^{\frac{2}{3}}}{z_i^{\frac{2}{3}}} = \frac{c_m S(z)}{\epsilon^{\frac{1}{3}}(kz_i)^{\frac{2}{3}}}\mathbf{E}(k,t)\times z_i z_i^{-1/3}\frac{w_*}{w_*} = \frac{c_m S(z) w_*}{(\epsilon z_i)^{1/3}(kz_i)^{\frac{2}{3}}}\mathbf{E}(k,t)\frac{z_i}{w_*} \\ &= \frac{c_m \phi_m u_*}{\kappa z}\frac{\psi_\epsilon^{-1/3}}{k'^{2/3}}\mathbf{E}(k',t_*)\frac{z_i}{w_*}\times\frac{w_*^2}{z_i^2}\frac{z_i^2}{w_*^2} = \left[\frac{c_m z_i^2 u_*}{w_*^2}\frac{\phi_m\psi_\epsilon^{-1/3}}{\kappa z k'^{2/3}}\mathbf{E}(k',t_*)\right]\frac{w_*}{z_i} = \mathbf{M}(k',t_*)\frac{w_*}{z_i}.\end{aligned} \tag{16}$$

2.2.3. Kinetic Energy Transfer by Inertial Effect

A turbulent flow is composed of eddies of different sizes or wavelengths. The small eddies are exposed to the field of tension generated by the big eddies. This stress field increases the vorticity of the small eddies and, consequently, their kinetic energy. This way, there is a transfer of turbulent kinetic energy from the biggest eddies to the smallest eddies until the Kolmogorov microscale is reached and energy dissipated as heat. This process is represented by the term $\mathbf{W}(k,t)$ in Equation (9) [5]. The same author suggests the use of the expression proposed by Pao [34] for an isotropic turbulent flow, which is given by the following equation:

$$\mathbf{W}_{iso}(k,t) = -\frac{\partial}{\partial k}\left[\alpha^{-1}\epsilon^{1/3}k^{5/3}\mathbf{E}(k,t)\right].$$

Performing the derivation and using the dimensionless variable:

$$\begin{aligned}\mathbf{W}_{iso}(k,t) &= -\frac{\partial}{\partial k}\left[\alpha^{-1}\epsilon^{1/3}k^{5/3}\mathbf{E}(k,t)\right] = -\alpha^{-1}\epsilon^{1/3}\frac{5}{3}k^{2/3}\mathbf{E}(k,t) - \alpha^{-1}\epsilon^{1/3}k^{5/3}\frac{\partial\mathbf{E}(k,t)}{\partial k} \\ &= -\alpha^{-1}\epsilon^{1/3}\frac{5}{3}k^{2/3}\mathbf{E}(k,t)\times\frac{z_i^{2/3}}{z_i^{2/3}} - \alpha^{-1}\epsilon^{1/3}k^{5/3}\frac{\partial\mathbf{E}(k,t)}{\partial k}\times\frac{z_i^{5/3}}{z_i^{5/3}} \\ &= -\alpha^{-1}\epsilon^{1/3}\frac{5}{3}(kz_i)^{2/3}\mathbf{E}(k,t)\frac{z_i^{1/3}}{z_i} - \alpha^{-1}\epsilon^{1/3}(kz_i)^{5/3}\frac{\partial\mathbf{E}(k,t)}{\partial k}\times\frac{z_i^{1/3}}{z_i^2} \\ &= -\frac{5}{3}\alpha^{-1}(\epsilon z_i)^{1/3}(kz_i)^{2/3}\mathbf{E}(k,t)\frac{1}{z_i}\times\frac{w_*}{w_*} - \alpha^{-1}(\epsilon z_i)^{1/3}(kz_i)^{5/3}z_i\frac{\partial\mathbf{E}(k,t)}{\partial k'}\frac{1}{z_i^2}\times\frac{w_*}{w_*} \\ &= -\frac{5}{3}\alpha^{-1}\frac{(\epsilon z_i)^{1/3}}{w_*}(kz_i)^{2/3}\mathbf{E}(k',t_*)\frac{w_*}{z_i} - \alpha^{-1}\frac{(\epsilon z_i)^{1/3}}{w_*}(kz_i)^{5/3}\frac{\partial\mathbf{E}(k',t_*)}{\partial k'}\frac{w_*}{z_i} \\ &= -\left[\frac{5}{3}\alpha^{-1}\psi_\epsilon^{1/3}(k')^{2/3}\mathbf{E}(k',t_*) + \alpha^{-1}\psi_\epsilon^{1/3}(k')^{5/3}\frac{\partial\mathbf{E}(k',t_*)}{\partial k'}\right]\frac{w_*}{z_i} = \mathbf{W}_{iso}(k',t_*)\frac{w_*}{z_i}.\end{aligned} \tag{17}$$

The inertial energy transfer term is related to a homogeneous but non-isotropic (anisotropic) turbulence. This situation occurs when the source term of convective energy is present ($\mathbf{H}(k,t)$) and represented by the expression $\mathbf{W}_{aniso}(k,t)$. According to [5], the following formulation is suggested for $\mathbf{W}_{aniso}(k,t)$:

$$\mathbf{W}_{aniso}(k,t) = -\frac{\partial}{\partial k}\left[\frac{c_2}{w_* z_i}\epsilon^{2/3}k^{1/3}\mathbf{E}(k,t)\right], \tag{18}$$

and similar to $\mathbf{W}_{iso}$, the dimensionless equation for the anisotropic condition is obtained:

$$\begin{aligned}\mathbf{W}_{aniso}(k,t) &= -\frac{\partial}{\partial k}\left[\frac{c_2\epsilon^{2/3}}{w_* z_i}\mathbf{E}(k,t)\right] = -\frac{c_2\epsilon^{2/3}}{w_* z_i}\frac{\partial}{\partial k}\left[\frac{\mathbf{E}(k,t)}{k^{-1/3}}\right] = \frac{-c_2\epsilon^{2/3}}{w_* z_i k^{-1/3}}\left[\frac{\mathbf{E}(k,t)}{3k} + \frac{\partial\mathbf{E}(k,t)}{\partial k}\right] \\ &= \frac{-c_2}{w_* z_i}\epsilon^{2/3}\frac{1}{3}(k)^{-2/3}\mathbf{E}(k,t)\times\frac{z_i^{2/3}}{z_i^{2/3}}\frac{w_*^2}{w_*^2} - \frac{c_2}{w_* z_i}\epsilon^{2/3}k^{1/3}\frac{\partial\mathbf{E}(k,t)}{\partial k}\times\frac{z_i^{1/3}}{z_i^{1/3}}\frac{w_*^2}{w_*^2}\frac{z_i}{z_i} \\ &= -\frac{c_2}{3}\frac{(\epsilon z_i)^{2/3}}{w_*^2}(kz_i)^{-2/3}\mathbf{E}(k',t_*)\frac{w_*}{z_i} - c_2\frac{(\epsilon z_i)^{2/3}}{w_*^2}(kz_i)^{1/3}\frac{\partial\mathbf{E}(k',t_*)}{\partial k'}\times\frac{w_*}{z_i} \\ &= \left[-\frac{c_2}{3}\psi_\epsilon^{2/3}(k')^{-2/3}\mathbf{E}(k',t_*) - c_2\psi_\epsilon^{2/3}(k')^{1/3}\frac{\partial\mathbf{E}(k',t_*)}{\partial k'}\right]\frac{w_*}{z_i} = \mathbf{W}_{aniso}b(k',t_*)\frac{w_*}{z_i}.\end{aligned} \tag{19}$$

In [5], the authors assume the coexistence of these terms of energy transfer, that is, $\mathbf{W}(k,t) = \mathbf{W}_{iso}(k,t) + \mathbf{W}_{aniso}(k,t)$ and dimensionless form [4,5,39,41]:

$$\mathbf{W}(k,t) = \mathbf{W}_{iso}(k,t) + \mathbf{W}_{aniso}(k,t) = \left[\mathbf{W}_{iso}(k',t_*) + \mathbf{W}_{aniso}(k',t_*)\right] \frac{w_*}{z_i} = \mathbf{W}(k',t_*) \frac{w_*}{z_i}. \quad (20)$$

The graphs for **H** and **W** (Equations (14) and (19)) are plotted in Figure 2 in a situation of CBL growth modeling. This graph outlines the behavior of the term $\mathbf{W}_{aniso}$ (Equation (18)) adopted to represent the inertial energy transfer in an anisotropic turbulent flow and has the peculiarity of becoming positive for certain wave numbers. The disparity of $\mathbf{W}_{aniso}$ and **H** magnitudes is also noted for low wave numbers, which leads to a surplus of energy in the atmosphere, which is a desirable feature to describe the growth phenomenon of CBL. In addition, the term $\mathbf{W}_{iso}$ (Equation (17)) is effective in transferring energy to the inertial subinterval [34].

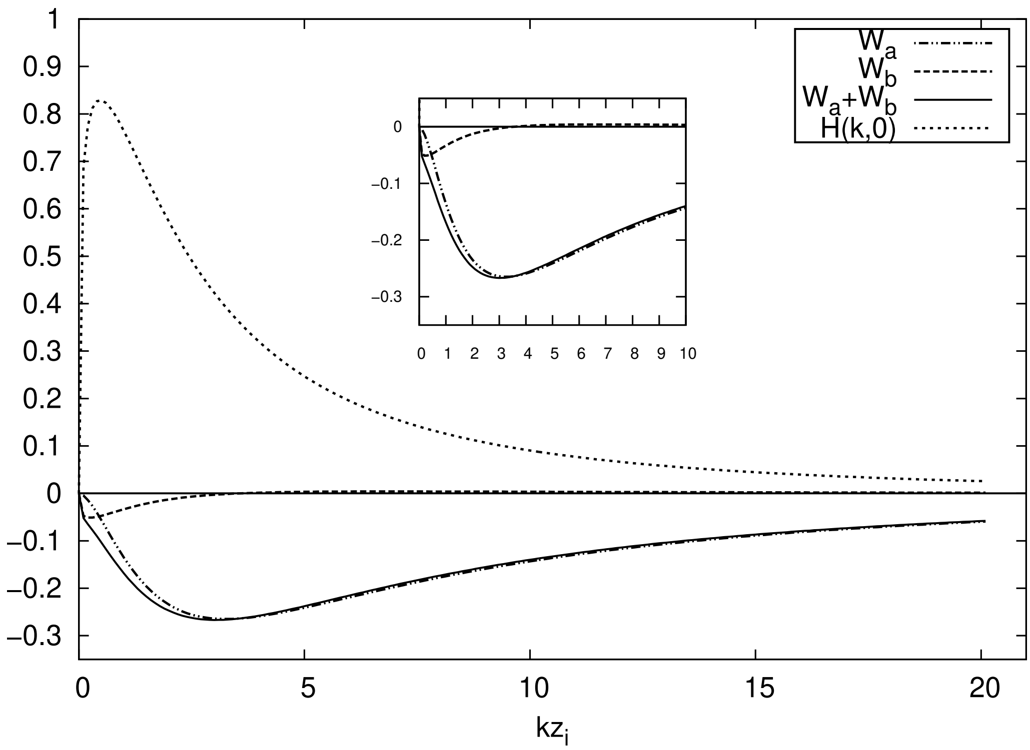

Figure 2. Graphical representation of the terms **H**, $\mathbf{W}_{aniso}$, $\mathbf{W}_{iso}$, and $\mathbf{W}_{iso} + \mathbf{W}_{aniso}$. Source: [4].

2.2.4. Energy Dissipation by Molecular Viscosity and Time Variation of the STKE: Dimensionless Equations

Turbulent flows are dissipative and require continuous energy input to compensate for viscous dissipation operated by the turbulent dissipation energy term ($-2\nu k^2 \mathbf{E}(k,t)$). Then, if there is no such energy replacement, turbulence decays rapidly and this term becomes responsible for TKE dissipation in CBL [2,33].

In this case, the dimensionless equation is given by:

$$-2\nu k^2 \mathbf{E}(k,t) = -2\nu k^2 \mathbf{E}(k,t) \times \frac{z_i^2}{z_i^2} \frac{w_*}{w_*} = -2\frac{\nu}{w_* z_i^2}(kz_i)^2 \mathbf{E}(k',t_*) \frac{w_*}{z_i} = -\frac{2}{R_e} k'^2 \mathbf{E}(k',t_*) \frac{w_*}{z_i}. \quad (21)$$

Using the temporal variation of energy ($\partial_t \mathbf{E}(k,t)$), the dimensionless form for Equation (9) is given by:

$$\frac{\partial\mathbf{E}\left(k,t\right)}{\partial t}=\frac{\partial\mathbf{E}\left(k,t\right)}{\partial t}\times\frac{z_i}{z_i}\frac{w_*}{w_*}=\frac{\partial\mathbf{E}\left(k',t_*\right)}{\partial\left(\frac{w_*}{z_i}t\right)}\frac{w_*}{z_i}=\frac{\partial\mathbf{E}\left(k',t_*\right)}{\partial t_*}\frac{w_*}{z_i} \tag{22}$$

2.3. The Evolution Equation for Dimensionless STKE

The results given by Equations (14), (16), (20)–(22) allow us to rewrite Equation (9) in the dimensionless form:

$$\frac{\partial\mathbf{E}\left(k',t_*\right)}{\partial t_*}=\mathbf{M}\left(k',t_*\right)+\mathbf{W}\left(k',t_*\right)+\mathbf{H}\left(k',t_*\right)-\frac{2}{R_e}k'^2\mathbf{E}\left(k',t_*\right), \tag{23}$$

more specifically, 1L-PDE is obtained by:

$$\frac{\partial\mathbf{E}(k',t_*)}{\partial t_*}+\left(c_2\psi_\epsilon^{2/3}(k')^{1/3}\right)\frac{\partial\mathbf{E}(k',t_*)}{\partial k'}+\left(\frac{c_2}{3}\frac{\psi_\epsilon^{2/3}}{(k')^{-2/3}}+\frac{2k'^2}{R_e}\right)\mathbf{E}\left(k',t_*\right)=\frac{w_*z_i\frac{\partial\theta}{\partial z}}{\left(\overline{w\theta}\right)_0}\frac{c_1\mathbf{E}_0(k')}{\psi_\epsilon^{1/3}(k')^{2/3}}\sin\left(\frac{z_i\Omega t_*}{w_*}\right). \tag{24}$$

When specifying an initial condition of the form: $\mathbf{E}_0\left(k'\right)=\mathbf{E}\left(k',t_0^*\right)$, the Cauchy Problem associated is:

$$\begin{cases}\frac{\partial\mathbf{E}(k',t_*)}{\partial t_*}+\left(c_2\psi_\epsilon^{2/3}(k')^{1/3}\right)\frac{\partial\mathbf{E}(k',t_*)}{\partial k'}+\left(\frac{c_2}{3}\frac{\psi_\epsilon^{2/3}}{(k')^{-2/3}}+\frac{2k'^2}{R_e}\right)\mathbf{E}\left(k',t_*\right)=\frac{w_*z_i\frac{\partial\theta}{\partial z}}{\left(\overline{w\theta}\right)_0}\frac{c_1\mathbf{E}_0(k')}{\psi_\epsilon^{1/3}(k')^{2/3}}\sin\frac{z_i\Omega t_*}{w_*} & .\\ \mathbf{E}_0\left(k'\right)=\mathbf{E}\left(k',t_0^*\right). & \end{cases} \tag{25}$$

The IC $\mathbf{E}_0\left(k'\right)=\mathbf{E}\left(k',t_0\right)$ is a three-dimensional STKE referred in previous section. Under the hypothesis of homogeneous and anisotropic turbulence, the theoretical tool developed by [3] can be used to create this I.C. from one-dimensional spectra, which can be obtained from experimental measurements or theoretical formulations.

2.4. First Order Linear PDEs

A general PDE of order k can be represented as

$$F\left(\mathbf{x},(\partial^\alpha u)_{|\alpha|\le k}\right)=0, \tag{26}$$

where F and u are functions of the variables $\mathbf{x}\in\Omega$ and $(u_\alpha)_{|\alpha|\le k}\in\mathbb{C}^{\mathbb{N}(k)}$, with Ω being an open set in $\mathbb{R}^n$ citefolland,szinvelskitese.

Given the linearity of the 1st-PDE, one can rewrite as

$$\sum a_j(\mathbf{x})\partial_j u+b(\mathbf{x})u=c(\mathbf{x}). \tag{27}$$

The PDE contained in System (25) falls in the form given by Equation (27) and consequently, PDE resolution methods given by Equation (27) are applied to the problems of STKE Evolution modeling. The Method of Characteristics that will be employed in the resolution of the Cauchy Problem (25) and in the following sections are presented in different approaches for the compression and manipulation of the respective method.

2.4.1. Method of Characteristics

The Method of Characteristics can be used as a strategy to break a PDE into a First Order ODE System. This process allows the description of the characteristic curves by a variable change that will condense the terms of the partial derivatives of u into a total derivative regarding this new variable, which in turn will anable the description of the characteristic curves depending on a single parameter and, thus, the PDE is transformed into ODE system.

The description above characterizes the method by the inherent simplicity of the construction (or non-construction) of the solution and simultaneously provides the demonstration path for the theorems of existence and local uniqueness for 1st-PDE solution. Furthermore, it allows a global understanding of the role of the initial or contour conditions for the question of the existence, uniqueness, and properties of the solution. An example of the application of this process in an EDP and description of their respective concepts involved in the solution construction are shown in Appendix A.

Another highlight of the method is the geometric parallel via interaction of the geometric properties of surfaces (or hypersurfaces) and vectors of the vector field associated with PDE. This allows a visualization of the interaction of the involved geometric entities in $\mathbb{R}^2$, and their conditions of applicability and properties that the entities must fulfill to determine the solution.

In order to expose this geometric bias, a 1L-PDEwas done in $\mathbb{R}^2$ in the form of the parameter equation

$$F\left(x, y, z, z_1, z_2\right) = 0 \Leftrightarrow a_1(x,y)z_1 + a_2(x,y)z_2 + b(x,y)z - c(x,y) = 0, \tag{28}$$

where $z = u(x, y)$ and the parameters $z_1 = u_x$ and $z_2 = u_y$.

In addition, it is assumed that there is an integral surface S in which a point $P_0 = (x(t_0) = x_0, y(t_0) = y_0, z(t_0) = z_0), t_0 \in I \subset \mathbb{R}$ is considered. At this point, vector direction V_{P_0} associated with PDE (Appendix A) is well defined. Hence, we will construct the integral curve $\mathcal{C} \doteq (x(t), y(t), z(t)) \subset S$ passing by P_0, which has as vector tangent $\mathbf{V}_{P_0}$.

First, this vector tangent to $\mathcal{C}$ (at any point $P \in \mathcal{C}$, as will be proved later) will belong to the tangent plane of the integral surface S(candidate to the surface solution), where the characteristic curve will be orthogonal to the normal vector $\left(z_x, z_y, -1\right)$: $(x(t), y(t), z(x(t), y(t)))\cdot\left(z_x, z_y, -1\right)$=0, for a given $t \in I \subset \mathbb{R}$.

One can determine a family of plans containing P_0, in which the tangent plane of the solution surface at P_0 and described in dependence on parameters z_1 and z_2 is included. Therefore, the relationship below is obtained by assuming $z_2 = z_2(z_1)$ $(a_2 \neq 0)$

$$\frac{dz_2}{dz_1} = -\frac{x - x_0}{y - y_0}.$$

On the other hand, the derivative in relation to z_1 from Equation (28) produces the direction field given by

$$\frac{x - x_0}{a_1} = \frac{y - y_0}{a_2} = \frac{z - z_0}{z_1 a_1 + z_2 a_2}. \tag{29}$$

Equation (29) defines the direction vector of the straight lines contained in the respective planes belonging to the family of tangent planes, and the union of all these generatrix straight lines and the point P_0 form the Monge Cone (Figure 3a) [6]. In this field of cones (Figure 3b), in all the generated plans , by specifying z_1 and z_2, a set of planes that surrounds the Monge cone is formed, only those containing the line defined by Equation (29) will be the tangent planes of the integral surface. In this maner, the integral surface will be tangent to a specified vertex cone P_0 with the curve, whose direction vector line is given by $(a_1, a_2, z_1 a_1 + z_2 a_1)$ (Figure 3).

To create the equivalent of the characteristic curve described above, it will require

$$\left(x'(t), y'(t), z'(t)\right) = \left(a_1, a_2, z_1 a_1 + z_2 a_2\right), \tag{30}$$

where the general form is given by $\left(x'(t), y'(t), z'(t)\right) = (F_{z_1}, F_{z_2}, z_1 F_{z_1} + z_2 F_{z_2})$.

The vector tangent for the curve candidate for the characteristic curve at P_0 has direction parallel to the direction vector of Monge cone and in which only one of these directions will represent the vector tangent to the $\mathcal{C}$ belonging to the plane tangent to the integral surface at P_0.

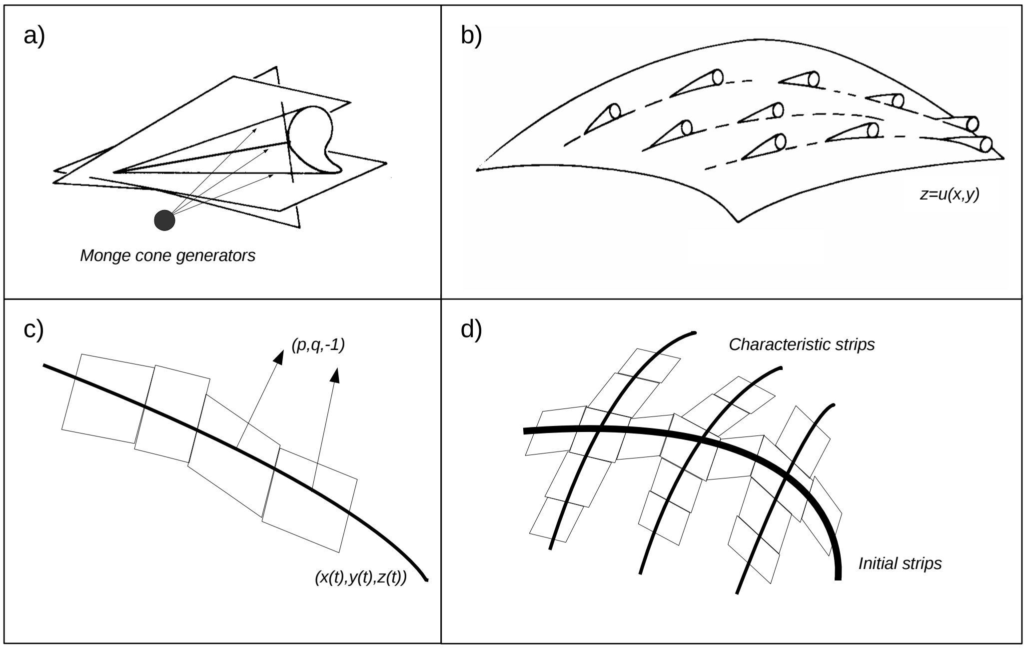

Figure 3. (**a**) *Monge Cone* and its forming planes. (**b**) Field of cones on the integral surface. (**c**) Geometric sketch of properties of the characteristic strip. (**d**) Construction of the characteristic strips from the initial strip and their respective support curves. Figure modified from the figures in ([6] (1981)—Figure 5ad).

The unknown z_1 and z_2 in the System given by Equation (30) do not allow the determination of the characteristic direction yet. For this, it is necessary to determine under what conditions do values $z_1(t_0)$ and $z_2(t_0)$ satisfy the condition that vector $(z_1(t_0), z_2(t_0), -1)$ is normal for the integral surface in addition to it requiring two equations to complete the System (30). Hence, in Equation (28), the derivative in relation to y produces

$$\partial_y (a_1 z_1 + a_2 z_2 + bz - c) = 0 \Leftrightarrow (z_2)_x a_1 + (z_2)_y a_2 = -(z_1 \partial_y(a_1) + z_2 \partial_y(a_2) + z\partial_y(b) + \partial_y(c) - z_2 b),$$

where $(z_1)_y = (z_2)_x$.

However, if (x_0, y_0, z_0) is in the integral surface, it follows

$$z_2{}'(t_0) = \frac{d}{dt} z_2(x(t), y(t))\Big|_{t=t_0} = (z_2)_x \frac{dx(t)}{dt}\Big|_{t=t_0} + (z_2)_y \frac{dy(t)}{dt}\Big|_{t=t_0} = -(z_1 \partial_y(a_1) + z_2 \partial_y(a_2) + z\partial_y(b) + \partial_y(c) + z_2 b)$$

in order that $z_2{}'(t_0) = -F_y - z_2 F_z$, which is and analogous to z_1': $z_1{}'(t_0) = -(z_1 \partial_x(a_1) + z_2 \partial_x(a_2) + z\partial_x(b) + \partial_x(c) + z_1 b)$.

Since t_0 is a generic value, the characteristic curves will be given by the characteristic system:

$$\begin{cases} x'(t) = a_1 = F_{z_1} \\ y'(t) = a_2 = F_{z_2} \\ z'(t) = z_1 a_1 + z_2 a_2 = z_1 F_{z_1} + z_2 F_{z_2} \\ z_1{}'(t) = -(z_1 \partial_x(a_1) + z_2 \partial_x(a_2) + z\partial_x(b) + \partial_x(c) + z_1 b) = -(F_x + z_1 F_z) \\ z_2{}'(t) = -(z_1 \partial_y(a_1) + z_2 \partial_y(a_2) + z\partial_y(b) + \partial_y(c) + z_2 b) = -(F_y + z_2 F_z) \end{cases},$$

This System contains the necessary conditions to determine the characteristic curve associated with Equation (28). Note that when determining one of these curves containing P_0, it was necessary to establish information about the plan (containing P_0) in which it resides, as this set (curve and plan in P_0) determines a characteristic strip (Figure 3c) and the characteristic curve is said support of this strip.

The characteristic strip will be created from an initial range that in turn, the construction of this initial strip will be similar to the construction of a characteristic strip. First, an initial support curve is created, $(\alpha(s), \beta(s), \phi(s))$ - the initial parameterized condition. This initial support curve should be contained by plans (Figure 3d) and, in any of these plans, will have as normal vector $(z_1(s), z_2(s), -1)$ for some particular s on the support curve:

$$a_1 z_1(s) + a_2 z_2(s) + b\phi(s) - c = 0 \Leftrightarrow F(\alpha(s), \beta(s), \phi(s), z_1(s), z_2(s)) = 0.$$

Note that there is an equation for two unknowns. The auxiliary condition arises from the fact that z must contain this initial curve ($z(\alpha(s), \beta(s)) = \phi(s)$, to $s \in I \subset \mathbb{R}$) and therefore, the auxiliary condition will be given by $\phi'(s) = z_x \alpha'(s) + z_y \beta'(s) = \alpha'(s) z_1(s) + \beta'(s) z_2(s)$.

The characteristic strip are First Order ODE System solutions

$$\begin{cases} \dfrac{dx(s,t)}{dt} = F_{z_1}(x(s,t), y(s,t)) \\ \dfrac{dy(s,t)}{dt} = F_{z_2}(x((s,t), y(s,t)) \\ \dfrac{dz(s,t)}{dt} = z_1(s,t) F_{z_1}(x(s,t), y(s,t)) + z_2(s,t) F_{z_2}(x(s,t), y(s,t)) \\ \dfrac{dz_1(s,t)}{dt} = -(F_x(s,t) + z_1(s,t) F_z(s,t)) \\ \dfrac{dz_2(s,t)}{dt} = -(F_y(s,t) + z_2(s,t) F_z(s,t)) \end{cases}, \tag{31}$$

with initial conditions

$$\begin{cases} x(s,t_0) = \alpha(s) \\ y(s,t_0) = \beta(s) \\ z(s,t_0) = f(s) \\ F(\alpha(s), \beta(s), \phi(s), z_1(s,t_0), z_2(s,t_0)) = 0 \\ \phi'(s) = \alpha'(s) z_1(s,t_0) + \beta'(s) z_2(s,t_0) \end{cases}. \tag{32}$$

The assumptions required for the existence and uniqueness of the solution of a first order ODE system are guaranteed by assuming that $a_1, a_2, z_1 a_1 + z_2 a_2, F_x + z_1 F_z, F_y + z_2 F_z, z_1$ and $z_2 \in C^1$. This result guarantees the existence and uniqueness of these characteristic strips [43,44].

The results and comments of this section are based on bibliographies: [6,45–47].

2.4.2. Local Existence and Uniqueness of Solution for a Linear First Order PDE

The previous section establisheds procedures and geometric relationships associated with solving the parameter equation represented for Equation (28).

For a First Order General PDE ($F : \Omega \times \mathbb{R} \times \mathbb{R}^n \rightarrow \mathbb{R}$ of class C^1 [47]) is:

$$F(x_1, \ldots, x_n, u, \partial_1 u, \ldots, \partial_n u) = 0. \tag{33}$$

Its equivalent in the form of a parameter equation is

$$F(x_1, \ldots, x_n, y, z_1, \ldots, z_n) \equiv \sum a_j(\mathbf{x}) z_j + b(\mathbf{x})\, y(\mathbf{x}) - c(\mathbf{x}) = 0. \tag{34}$$

where they are associated by $y = u(\mathbf{x})$ and $z_j = \partial_j u$, $\Omega \subset \mathbb{R}^n$, an opening solution domain of Equation (33).

And the equivalent of System (31) and (32) for this situation is:

$$\begin{cases} \dfrac{dx_j}{dt} = \dfrac{\partial F}{\partial z_j} = a_j(\mathbf{s},t) \\ \dfrac{dy}{dt} = \sum z_j a_j(\mathbf{s},t) = \sum z_j a_j(\mathbf{s},t) \\ \dfrac{dz_j}{dt} = -\dfrac{\partial F}{\partial x_j} - z_j \dfrac{\partial F}{\partial y} \\ \quad \mathbf{x}(\mathbf{s},0) = \gamma(\mathbf{s}), \quad y(\mathbf{s},0) = \phi(\gamma(\mathbf{s})) \\ \dfrac{\partial y}{\partial s_j} = \sum z_k \dfrac{\partial \gamma_k}{\partial s_j} \Leftrightarrow \partial_{s_k}\phi(g(\mathbf{s})) = \partial_{s_k}\gamma(\mathbf{s}) z_j(\mathbf{s},0) \\ \quad F(\gamma(\mathbf{s}), \phi(\gamma(\mathbf{s})), z_j(\gamma(\mathbf{s}))) = 0 \end{cases}, \tag{35}$$

and from it, x_j, y, and z_j are obtained as functions of $\mathbf{s}$ and t [4,10].

Coordinate change (as described in the molds of Appendix A) will be ensured by observing some conditions related to the initial condition associated with the problem, more specifically if γ is a Non-Characteristic Hypersurface. Thus, for $z_1, \ldots, z_n \in C^1$ satisfying the last two equations of System (35) over γ leads

$$\left\| \begin{matrix} \frac{\partial x_1}{\partial s_1} & \cdots & \frac{\partial x_1}{\partial s_{n-1}} & \frac{\partial x_1}{\partial t} \\ \vdots & \ddots & \vdots & \vdots \\ \frac{\partial x_n}{\partial s_1} & \cdots & \frac{\partial x_n}{\partial s_{n-1}} & \frac{\partial x_n}{\partial t} \end{matrix} \right\| \neq 0. \tag{36}$$

Therefore, by the implicit function theorem, in a neighborhood of P_0, there are the functions $\mathbf{s} = \mathbf{s}(\mathbf{x})$ and $t = t(\mathbf{x}) \in C^1$, such that locally $\mathbf{x} = \mathbf{x}(\mathbf{s},t)$ is valid.

Nevertheless, the System formed above has a unique solution for y under the validity of Equation (33) [43,44]. However, it should be noted that the existence of solution u is not guaranteed, as the expression $y = u(\mathbf{x})$ has not yet been validated.

The first step in this validation will be to verify the existence of an inverse coordinate transformation $(\mathbf{s},t) \mapsto \mathbf{x} = \mathbf{x}(\mathbf{s},t)$, such that $t = t(\mathbf{x}) \in C^1$. Notwithstanding, condition given by Equation (36) ensures that the mapping can be reversed, in order that $\mathbf{s}$ and $t \in C^1$ are functions of $\mathbf{x}$ around a neighborhood of $P_0 \in \gamma$ ensures the uniqueness of the solution of an ODE system in this vicinity of P_0 [43,44]

Thus far, only $y = y(\mathbf{s}(\mathbf{x}), t(\mathbf{x}))$ has been obtained. To ensure the existence and uniqueness of the solution u of Equation (33), $y(\mathbf{s}(\mathbf{x}), t(\mathbf{x})) = u(\mathbf{x})$ must be shown to satisy Equation (34) and $z_j = \partial_j u(\mathbf{x})$.

In fact, if $y = u(\mathbf{x}) = u(\mathbf{s},t)$, then u

i. satisfies IC: $u(\gamma(\mathbf{s})) = y(\mathbf{s}(\mathbf{x}),0) = \phi(\gamma(\mathbf{s}))$. Indeed, $\Gamma : u|_\gamma = \phi \Leftrightarrow \mathbf{x}(\mathbf{s},0) = \gamma(\mathbf{s})$ and $y(\mathbf{s},0) = \phi(\gamma(\mathbf{s}))$, where for the purposes of simplifying notation, it is assumed that $t_0 = 0$;

ii. around Γ, given $\mathbf{s}_0$, one has

$$\partial_t F(\mathbf{x}(\mathbf{s},t), u(\mathbf{s},t), z_j(\mathbf{s},t)) = \sum F_{x_j}\partial_t x_j + F_u u_t + \sum F_{z_j}\partial_t z_j = \sum F_{x_j} a_j + \sum z_j a_j + \sum a_j \left(-F_{x_j} - z_j\right) = 0.$$

with the initial condition given by:

$$F(\mathbf{x}(\mathbf{s},0), u(\mathbf{s},0), z_j(\mathbf{s},0)) = 0 \therefore F(\mathbf{x}(\mathbf{s},t), u(\mathbf{s},t), z_j(\mathbf{s},t)) = 0.$$

Thus, if the characteristic curve has a point in common with the integral surface, the entire curve will be contained in it;

iii. Given $u_{\mathbf{x}}$, according to the Chain Rule, we obtain:

$$\begin{cases} u_{s_k} = \sum_{j=1}^{n} \frac{\partial u}{\partial x_j}\frac{\partial x_j}{\partial s_k},\ k = 1, \ldots, (n-1) \\ u_t = \sum_{j=1}^{n} \frac{\partial u}{\partial x_j}\frac{\partial x_j}{\partial t} \end{cases}, \tag{37}$$

The matrix associated with this system is the Jacobian Matrix itself: $\begin{pmatrix} \frac{\partial x_1}{\partial s_1} & \cdots & \frac{\partial x_1}{\partial s_{n-1}} & \frac{\partial x_1}{\partial t} \\ \vdots & \ddots & \vdots & \vdots \\ \frac{\partial x_n}{\partial s_1} & \cdots & \frac{\partial x_n}{\partial s_{n-1}} & \frac{\partial x_n}{\partial t} \end{pmatrix}$, which has non-zero determinant due to its Non-Characteristic Condition. Thus, the above System has a unique solution;

iv. From the second equation of System (35), we have: $u_t = \sum \frac{\partial u}{\partial x_j}\frac{dx_j}{dt} = \sum z_j F_{z_j} = \sum z_j a_j$.

The first equation of System (37) is derived from t, as follows:

$$\begin{aligned} \partial_t\left[u_{s_k} - \sum z_j \partial_{s_k} x_j\right] =& \partial_t\left[u_{s_k} - \sum z_j \partial_{s_k} x_j\right] - 0 = \partial_t\left[u_{s_k} - \sum z_j \partial_{s_k} x_j\right] - \partial_{s_k}\left[u_t - \sum z_j \partial_t x_j\right] \\ =& u_{ts_k} - \sum \partial_t z_j \partial_{s_k} x_j - \sum z_j \partial_{ts_k} x_j - u_{s_k t} + \sum \partial_{s_k} z_j \partial_t x_j + \sum z_j \partial_{s_k t} x_j \\ =& -\sum \partial_t z_j \partial_{s_k} x_j + \sum \partial_{s_k} z_j \partial_t x_j = \sum\left(-\partial_{x_j} F - z_j F_u\right)\partial_{s_k} x_j + \sum \partial_{s_k} z_j \partial_{z_j} F \\ =& \sum z_j F_u \partial_{s_k} x_j + \sum \partial_{x_j} F \partial_{s_k} x_j + \sum \partial_{s_k} z_j \partial_{z_j} F \\ =& \sum z_j F_u \partial_{s_k} x_j - F_u u_{s_k} - \sum F_{z_j} \partial_{s_k} z_j + \sum \partial_{s_k} z_j \partial_{z_j} F - \left(u_{s_k} - \sum z_j \partial_{s_k} x_j\right) \\ =& \left(\sum z_j \partial_{sk} x_j - u_{s_k}\right). \end{aligned}$$

Naming $H(\mathbf{s}, t) = \{u_{s_k} - \sum z_j \partial_{s_k} x_j$, there is a System of $(n-1)$ ODEs synthesized by

$$\partial_t H(\mathbf{s}, t) = -H(\mathbf{s}, t),$$

whose solution is $H(\mathbf{s}, t) = H(\mathbf{s}, 0)\exp(-t)$.

Note that the associated initial condition is given by: $H(\mathbf{s}, 0) = \phi'(\gamma(\mathbf{s})) - \sum \gamma'(\mathbf{s}) z_j(\mathbf{s}, 0) = 0$, therefore $H(\mathbf{s}, t) = \mathbf{0}$ and unique. With this,

$$\begin{cases} u_{s_k} = \sum z_j \partial_{s_k} x_j,\ k = 1, \ldots, (n-1) \\ u_t = \sum z_j \partial_t x_j \end{cases}.$$

Since z_j is a solution of this System (for the same reasons as System (37)), it follows that $z_j = u_{x_j}$ is for $j = 1, \ldots, n$.

Thus, $u(\mathbf{x}) = y(\mathbf{s}(\mathbf{x}), t(\mathbf{x}))$ simultaneously satisfies the linear versions of Equations (33) and (34), as $u = \phi$ in γ and items *i*, *ii*, *iii*, and *iv* above. As a result, the existence and uniqueness of u defined in an open $\Omega \subset \mathbb{R}^n$ is valid. The preceding discussion is, in fact, a commented demonstration of the following theorem:

Theorem 1 (Local Existence and Uniqueness of Solution for a Linear PDE)**.** *Suppose γ is a hypersurface of class C^1 at Ω, which is non-characteristic: $\left(a_1(\mathbf{x}), \ldots, a_n(\mathbf{x})\right)$ is non-tangentγ, $\forall\, \mathbf{x} \in \gamma$ (see Condition (36)) and that a_j, b, c are real functions of class $C^1(\Omega)$ and ϕ of class $C^1(\gamma)$. Therefore, for any small enough* *neighborhood of Ω' of γ in $\mathbb{R}^n$, there is a single solution $u \in C^1(\Omega)$ of $\sum_j a_j(\mathbf{x})\partial_j u + b(\mathbf{x})u = c(\mathbf{x})$, Ω satisfies $u = \phi$ over γ.*

3. Isotropic Model

In an isotropic turbulent flow, the dynamic equation for the STKE is obtained by disregarding the terms of energy production by mechanical effect $\mathbf{M}(k', t_*)$ and energy production or loss by thermal effect $\mathbf{H}(k', t_*)$. In this case, the CBL represents a typical convective turbulence decay situation, in which the TKE generating structures have been deactivated, that is, they are no longer acting. Consequently, a fully developed CBL turbulence regime is assumed in the sense that time and length scales and other constituent parameters are present in the formulation of the initial three-dimensional spectrum, which will represent the initial condition of the proposed isotropic model.

This simplified model is formulated considering the TKE transfer and dissipation processes at the Planetary Limit Layer (PBL). The transfer of the kinetic energy mechanism will act as described in Section 2.2.3, where TKE will transfer from the biggest eddies to the smallest ones until the Kolmogorov microscale is reached and energy dissipated as heat. In practice, this model can be employed, through some adaptations, in the sunset period and windless condition after a fully developed CBL.

Under these assumptions, the initial spectrum is obtained according to the technique suggested by [3] from the one-dimensional spectrum F_u, F_v, and F_w as a function of n and k with $k = \dfrac{2\pi n}{U}$, as suggested by [16] and other similar studies, including [48]. The isotropic limit condition of this constructive process is given by

$$\mathbf{E}_0(k') = (k')^3 \frac{d}{dk'}\left(\frac{1}{k'}\frac{dF_u}{dk'}\right) = \frac{5a_u b_u k' \left(3 + 11 b_u k'\right)}{9\left(1 + b_u k'\right)^{11/3}}, \tag{38}$$

and F_u represents the unidimensional spectrum associated with velocity u (Appendix B).

Equation (23) can be written as follows:

$$\frac{\partial \mathbf{E}(k', t_*)}{\partial t_*} = \mathbf{W}_{iso}(k', t_*) - \frac{2}{R_e} k'^2 \mathbf{E}(k', t_*)\,. \tag{39}$$

By replacing $\mathbf{W}_{iso}(k', t_*)$ given by Equation (17), Equation (39) gives the dimensionless equation,

$$\frac{\partial \mathbf{E}(k',t_*)}{\partial t_*} + \frac{\psi_\epsilon^{1/3}(k')^{5/3}}{\alpha}\frac{\partial \mathbf{E}(k',t_*)}{\partial k'} + \left(\frac{5\psi_\epsilon^{1/3}}{3\alpha}(k')^{2/3} - \frac{c_m z_i^2 u_*}{w_*^2}\frac{\phi_m \psi_\epsilon^{-1/3}}{\kappa z}k'^{-2/3} + \frac{2}{R_e}k'^2\right)\mathbf{E}(k', t_*) = 0. \tag{40}$$

The IVP is constructed by considering the initial condition: $\mathbf{E}_0\left(k'\right) = \mathbf{E}\left(k', t_0^* = 0\right)$.

Equation (40) is solved by the Method of Characteristics, where the ODE described in System (35) will be used to obtain the appropriate variable change [7]:

$$1 \cdot dk' - A(k')^{5/3} dt_* = 0 \Leftrightarrow \quad cte = At_* + \frac{3}{2}(k')^{-2/3} \quad (A = \alpha^{-1}\psi_\epsilon^{1/3}).$$

Changing the variable t_* to the parameter r and $cte = \frac{3}{2}s^{-2/3}$, obtains: $\begin{cases} r = t_* \\ k' = \left(s^{-2/3} - \dfrac{2}{3}Ar\right)^{-3/2} \end{cases}$

Therefore, the sought variable change is: $T : \begin{cases} r = t_* \\ s = \left(k'^{-2/3} + \dfrac{2}{3}At_*\right)^{-3/2} \end{cases} \Leftrightarrow \quad T^{-1} : \begin{cases} t_* = r \\ k' = \left(s^{-2/3} - \dfrac{2}{3}Ar\right)^{-3/2} \end{cases}.$

Where, $\dfrac{\partial(s, r)}{\partial(k', t_*)} = \left\| \begin{matrix} s_{k'} & s_{t_*} \\ r_{k'} & r_{t_*} \end{matrix} \right\| = k'^{-2/3} + \dfrac{2}{3}At_* \neq 0\,.$

This variable change allows us to write: $\mathbf{E}(k', t_*) = V(s, r)$, in fact: $\dfrac{dV}{dr} = \dfrac{\partial \mathbf{E}}{\partial t_*} + Ak'^{5/3}\dfrac{\partial \mathbf{E}}{\partial k'}$.

By applying the transformation to the new variables, we have the ODE and its initial condition:

$$\begin{cases} \dfrac{dV(s,r)}{dr} + \left[B\left(s^{-2/3} - \dfrac{2}{3}Ar\right)^{-1} + C\left(s^{-2/3} - \dfrac{2}{3}Ar\right)^{-3}\right] V(s,r) = 0, \\ V(s, r=0) = E_0 \end{cases} \tag{41}$$

where $B = \dfrac{5}{3}\alpha^{-1}\psi_\epsilon^{1/3}$ e $C = \dfrac{2}{R_e}$.

Solving the Cauchy Problem in System (41), the final solution is obtained:

$$\mathbf{E}(k', t_*) = \mathbf{E}_0 \left(\frac{1}{\left(k'^{-2/3} + \frac{2}{3}At_*\right)^{3/2}}\right)\left[\frac{k'}{\left(k'^{-2/3} + \frac{2}{3}At_*\right)^{3/2}}\right]^{-5/3} \exp\left\{-\frac{3C}{4A}\left[k'^{4/3} - \left(k'^{-2/3} + \frac{2}{3}At_*\right)^{-2}\right]\right\}. \tag{42}$$

According to Figure 4, the evolution of the spectral peacks show the rapid decrease of TKE in the temporal evolution of the model, a fact theoretically predicted for a PBL without TKE insertion mechanisms [2].

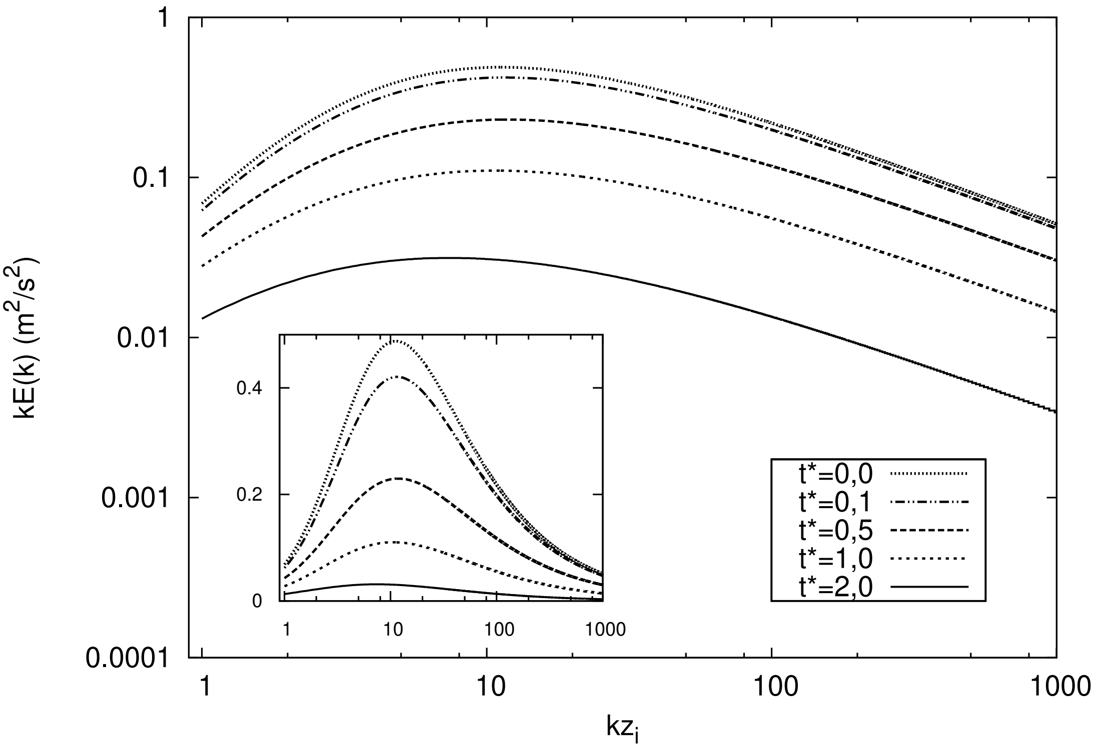

Figure 4. Calculated three-dimensional energy spectrum of Equation (42).

This model and resolution process can be found in [49,50], althought without the detail exposed here.

4. Final Considerations

The present study developed an introductory description of the evolution of STKE in CBL. This review article gives the reader a general, even simplified, view of the STKE modeling process. The initial assumption of buoyancy of the velocities of a turbulent flow allows its quantification through the autocorrelation function and posterior association via Fourier transform with the spectral density function under the hypothesis of a homogeneous turbulence. From this pair of functions, qualitative and quantitative information concerning the dynamics of the physical processes involved is extracted, and therefore, quantitative parameters typical of a turbulent flow can be obtained (time, length, and velocity scales [9,11,14–17]) , which are commonly employed in expressions to calculate, for example, lateral dispersion parameter and eddy diffusivities [16,51].

This study is far from being a complete work on the subject, since the process and techniques to deduce Equation (9) [1] and develop three-dimensional spectrum was not presented [3]. Nevertheless, this paper brings forward a guide for the commom concepts, techniques, and procedures employed in research related to the evolution of STKE in CBL, in addition to providing a basic bibliographic reference for the present theme.

The STKE defined via the Fourier transform of the autocorrelation function allows one to describe turbulent energy dynamic processes through frequency and/or wave number decomposition. The idea of a turbulent flux composed of interagency eddies on the various sizes and frequency scales suggests that the process is random in the three spatial directions and in time, which characterizes turbulence as a three-dimensional and temporal phenomenon [2]. In this manner, one-dimensional spectra do not contemplate the all information on the phenomenon of turbulence in the CBL and, for certain ranges of wave number values of the spectrum, the phenomenon of aliasing can occur [2], which will not take place in three-dimensional spectrum.

The spectral dynamics is described by Equation (9), which is an idealized model of the process involved in the evolution of TKE in the CBL. A brief description of the constituent parameters is presented with its respective bibliographic references. As an example, a simplified model was formulated under the hypothesis of isotropic turbulence acting on the entire wave number vector domain. In this model, the effective terms that govern this dynamic are the kinetic energy transfer by inertial effect ($\mathbf{W}_{iso}$) and viscous dissipation. Under these considerations, Equation (9) is a linear first order PDE, which evidences the relevance of the parametrization of the terms involved in the model since they will not only indicate the reliability of the model, but also influence the choice of the mathematical methods (analytical and/or numerical) to obtain the solution. To complement the model, it is necessary to inform an initial condition. For this, the techniques in [3] were used to develop an initial three-dimensional energy spectrum [4].

The simplified model solution is obtained by the Method of Characteristics. This method consists of obtaining characteristic curves in which the partial derivatives of the PDE are described as a total derivative, that is, the Method of Characteristics transforms an IVP to PDE in an IVP for ODE system. The description of this transformation process is detailed here and, evidence the geometric procedures in the construction of the method, which also indicates existence and uniqueness of the solution.

The solution obtained for this simplified model is shown in Figure 4. It represents the evolution of STKE proposed by the Cauchy Problem (41) and the rapid decrease of TKE in the temporal evolution of the model is observed. This result agrees with the expected behavior for a model that consider processes of transfer and dissipation of TKE without continuous TKE insertion sources (thermal convection and shear) in a PBL [2].

Therefore, the information and results obtained in this study may be suitable for the comprehension of turbulent kinetic energy dynamics in the convective boundary layer and, consequently, for applications in Eulerian and Lagrangian dispersion models.

Author Contributions: C.R.P.S. and L.B. wrote the manuscript. G.A.D. supervised, mentored, and advised all the research work that led to this paper. O.C.A. supervised the research work. G.A.D., T.T. and D.R.R. reviewed the manuscript and conducted the English editing.

Funding: The authors acknowledge the National Council for Scientific and Technological Development (CNPq, Brazil), the Coordination for the Improvement of Higher Education Personnel (CAPES, Brazil), Foundation for Research of Rio Grande do Sul State (FAPERGS) for their financial support.

Acknowledgments: The authors would like to thank the UFSM, PPGFIS-UFSM, Mathematics Department—UFSM.

Conflicts of Interest: The authors declare no conflict of interest.

Abbreviations

The following abbreviations are used in this manuscript:

STKE	Spectral Density Turbulent Kinetic Energy Equation
TKE	Turbulent Kinetic Energy
CBL	Convective Boundary Layer
3D-STKE	Three-Dimensional Energy Spectrum
PDE	Partial Differential Equation
PBL	Planetary Boundary Layer
1L-PDE	Linear First Order Partial Differential Equation
1st-PDE	First Order Partial Differential Equation
ODE	Ordinary Differential Equation
IC	Initial Condition
IVP	Initial Value Problem

Appendix A

To illustrate the application of the featured method, the 1-D Equation of Advection will be considered:

$$u_t + cu_x = 0,\; c \in \mathbb{R}. \tag{A1}$$

Equation (A1) is a 1L-PDE, such as Equation (24) and its solution will be made from geometric view.

Firstly, suppose there is the solution u of Equation (A1). The graph associated with u is the set $S \doteq \{x, t, u(x,t)\}$ and at each point (x,t), the value of the normal vector of S is given by $\hat{\mathbf{n}} = (u_x, u_t, -1)$.

From Equation (A1), we extract the vector $\mathbf{V} = (1, c, 0)$ and observe the orthogonality of the direction field and the normal vector $\hat{\mathbf{n}}$ of S, the graph of the solution u, that is $\mathbf{V} \cdot \hat{\mathbf{n}} = 0$. Therefore, $(1, c, 0)$ is perpendicular to $(u_x, u_t, -1)$ at each point $(x, t, u(x, y))$ and $(1, c, 0)$ belongs to the tangent plane to S (Figure A1a).

The tip for building u is to look for S at each point (x, t, z) of S, the vector $(1, c, 0)$ belongs to the tangent plane of S in (x, t, z) and $z \equiv u(x, t)$ [6,45,52].

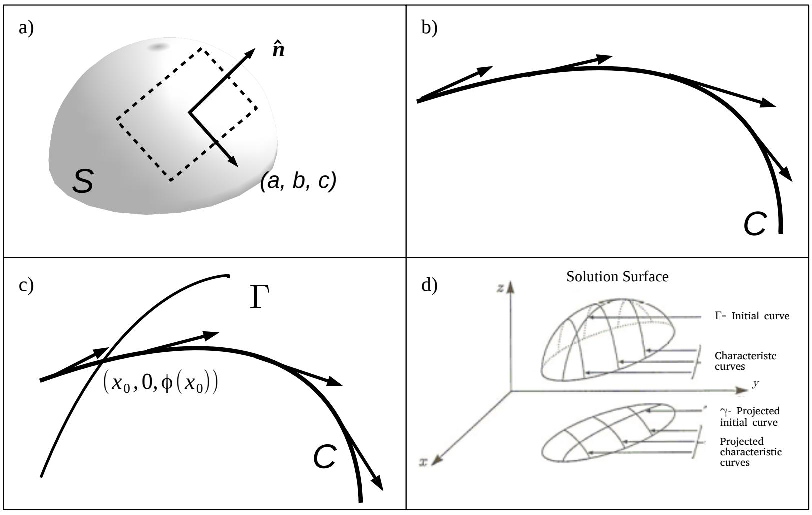

Figure A1. (**a**) Geometric sketch of vector field **V** and the normal vector $\hat{\mathbf{n}}$ of S ($\mathbf{V} \subset$ Tangent Plane to S). (**b**) Geometric representation of the integral curve $\mathcal{C}$. (**c**) Geometric design of the integral surface construction. (**d**) Solution surface generated by the initial curve Γ and its characteristic curves $\mathcal{C}$. Figure modified from Levandosky's figures ([52] (2002)—Figure 3a–c); and ([7] (2001)—Figure 3d).

For Equation (A1), the associated characteristic system is given by:

$$\left(\frac{dx(s,r)}{dr}, \frac{dt(s,r)}{dr}, \frac{dz(s,r)}{dr}\right) = (c, 1, 0). \tag{A2}$$

The geometric idea of the method is to construct the integral surface S, in order that it contains the curve $\Gamma := \{x, 0, \phi(x)\} \equiv \{\gamma, \phi(x)\}$, where γ is the plane projection of the initial curve Γ. From it, the characteristic curves that assemble S are obtained. For this, we consider the point of intersection of $\mathcal{C}$ and Γ, namely $(x_0, 0, \phi(x_0))$ (Figure A1c), then we can use

$$(x(s,0),\ t(s,0),\ z(s,0)) = (x_0, t_0, \phi(x_0)) \tag{A3}$$

as initial conditions for System (A2). At first, x_0 is any, which is valid considering the x-axis as an auxiliary curve and, algebraically, represents the parameter s, with which the initial curve is parameterized.

Thus, the Characteristic System formed by System (A2) and (A3),and the solution is given by:

$$(x(s,r), t(s,r), z(s,r)) = (c\,r + s, r, \phi(s)) \tag{A4}$$

The set of systems above represents the integral surface S consisting of the union of all the characteristic curves parameterized by the equations contained in the System (A4).

However, the solution is given in the parameters r and s and, to rewrite this solution in function of the variables x and t, we considered the first two equations of System (A4) to obtain $r(x,t)$ and $s(x,t)$. More specifically,

$$\begin{cases} s(x,t) = x - c\,t \\ r(x,t) = t \end{cases} . \tag{A5}$$

Consequently, a biunivocal transformation was established between the coordinate systems (x,t) and (r,s). When this transformation satisfies the Inverse Application Theorem [53], the change of variables is of class C^1. In this scenario, we can locally guarantee the existence and uniqueness of the solution, which is given by the integral surface constructed:

$$u(x,t) \equiv z(s(x,t), r(x,t)) = \phi(x - c\,t). \tag{A6}$$

System (A5) represents the projection of the characteristic curves found in an open $\Omega \subseteq \mathbb{R}^2$ (where $\gamma \subseteq \Omega$), in this case, the projected characteristic curves (Figure A1d).

Equation (A6) is a solution of an ODE and, in a way, it can be synthesized that the Method of Characteristics transforms an Initial Value Problem for PDE into an Initial Value Problem for ODEs via diffeomorphism (let U and V be open from Euclidean space. A bijection $f : U \to V$, is called diffeomorphism of U on V when f is differentiable and its inverse $f^{-1} : V \to U$ is also differentiable [53] (p. 277)).

Figure A2 shows the solution graph of the One-Dimensional Diffusion Equation given by Equation (A1) for $c = 2$, $x_0 = -155$, and $\phi(x) = 1 + \exp\left(\frac{-x^2}{10{,}000}\right)$ in the domain $(x,t) \in \Omega := \mathbb{R} \times (0, \infty)$.

The considerations in this section are basically a mixture of approaches and expositions of the first-order PDE by Method of Characteristics methodology from [7,45,52].

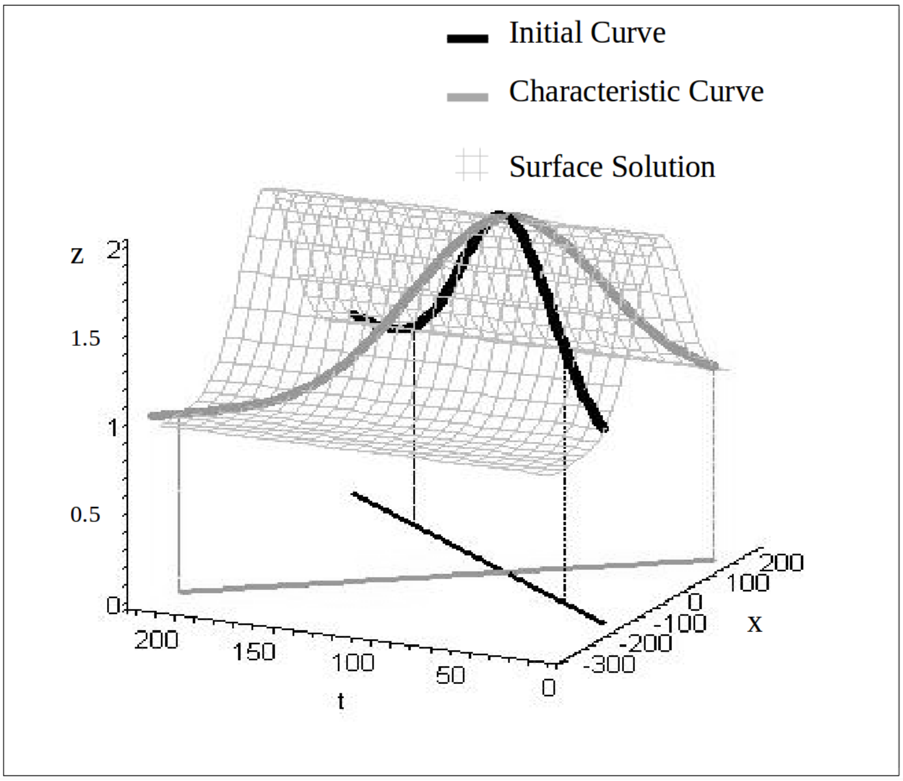

Figure A2. Graphical representation of the solution of Equation (A1), its initial curve, its characteristic curve and the respective plane projections.

Non-Characteristic Condition

The idea of the method presented in the previous section consists of satisfying a transversality condition for the initial condition $\Gamma := (\gamma, \phi)$ and the characteristic curves [10], where γ is assumed to be non-characteristic. *The initial condition should not be a characteristic hypersurface, that is, that the vectors of the direction field at a point P of the hypersurface γ are not tangent to γ in P.*

The first-order PDE given by Equation (A1) is the simplest possible situation (linear, homogeneous, and with constant coefficients), even though it exhibits dependence of existence, uniqueness, and properties in the solution in relation to the initial data, as shown below

i. *The initial curve is a characteristic curve.*

In this case, $\gamma \doteq x - ct = 0 \Rightarrow (cs, s)$, $s \in I \subset \mathbb{R}$ and considering the solution of the system: $\begin{cases} x(r,s) = c\,r + c_1(s),\ x(r=0,s) = cs \\ t(r,s) = r + c_2(s),\ t(r=0,s) = s \end{cases}$ is given by $\begin{cases} x(r,s) = c\,r + c\,s \\ t(r,s) = r + s \end{cases}$.

In order to obtain the bijection, we solve r and s as a function of (x, t), although the system does not allow this inversion. From it we only obtain that x–ct=0, and then $z = \phi(s)$Additionally, if $z = \phi(0)$ is constant, there are inumerous solutions to the problem. If IC: $\phi(s) = f(s)$, with non-constant f the problem does not admit solution [7].

ii. If γ *with tangent vectors parallel to the tangent vectors of the projected characteristic curve.*

Let, IC $\doteq x - \frac{c}{2}t^2 = 0 \Rightarrow (\frac{c}{2}s^2, s)$, $s \in I \subset \mathbb{R}$. At $s = 1$ the tangent vectors of the characteristic curve and the initial curve are parallel. In this situation, a solution is obtained for r and for s, in the form: $s = 1 \pm \sqrt{1 + \frac{2}{c}(x - ct)}$ and $r = t - 1 \mp \sqrt{1 + \frac{2}{c}(x - ct)}$, since $x - ct \geq -\frac{c}{2}$.

These *anomalous situations* are because projected characteristic curves and γ has parallel tangent vectors in their domains. To avoid this, the initial condition must satisfy the *Non-Characteristic Condition*.

From System (A2), we have the product: $(1, c) \cdot (-0, 1) = \begin{Vmatrix} 1 & 1 \\ 0 & c \end{Vmatrix} = c \neq 0$, $\forall r \in I \subset \mathbb{R}$, that is, the tangent vectors of γ are not parallel to the projected direction field vectors (which form the characteristic curves) defined on a point P in Γ, in order that they do not belong to the tangent plane of γ in P_γ. However, if they do not belong to the tangent plane of γ in P_γ, then the vectors of the direction field are not orthogonal to the normal field of γ in P_γ. For the general case, $F\left(\mathbf{x}, u, \partial_1 u, \ldots, \partial_n u, \partial_1^2 u, \ldots, \partial_n^k u\right) = 0$, generalization is immediate

$$\nabla_{\mathbf{z}} F(\Gamma(\mathbf{s}), z_j(g(\mathbf{s}))) \cdot N(\gamma(\mathbf{s})) \neq 0 \Leftrightarrow \begin{Vmatrix} \frac{\partial \gamma_1}{\partial s_1} & \cdots & \frac{\partial \gamma_1}{\partial s_{n-1}} & \frac{\partial F}{\partial z_1}\left(\gamma(\mathbf{s}), \phi\left(\gamma(\mathbf{s})\right), z_j\left(\gamma(\mathbf{s})\right)\right) \\ \vdots & \ddots & \vdots & \vdots \\ \frac{\partial \gamma_n}{\partial s_1} & \cdots & \frac{\partial \gamma_n}{\partial s_{n-1}} & \frac{\partial F}{\partial z_n}\left(\gamma(\mathbf{s}), \phi\left(\gamma(\mathbf{s})\right), z_j\left(\gamma(\mathbf{s})\right)\right) \end{Vmatrix} \neq 0, \quad \text{(A7)}$$

where $N(\gamma(\mathbf{s}))$ represents the normal field of the initial hypersurface γ of dimension n.

Appendix B. Parameterization Employed in the Construction of Three-Dimensional Spectrum

The one-dimensional Eulerian spectra employed in the construction of $\mathbf{E}_0$ are given by [16,48]

$$\frac{n\, S_i^E(n)}{w_*^2} = \frac{1.06\, c_i\, f\, \psi_\epsilon^{2/3} \left(\frac{z}{z_i}\right)^{2/3}}{(f_m^*)_i^{5/3} \left[1 + 1.5 \left(\frac{f}{(f_m^*)_i}\right)\right]^{5/3}},$$

where:

- z is the height above the ground and z_i is the top of the CBL and n is the frequency;
- $c_i = \alpha_i \alpha_u \left(2\pi\kappa\right)^{-2/3}$; α_i is derived experimentally from the spectrum for each wind direction components, and is 1, $\frac{4}{3}$ and $\frac{4}{3}$ to u-longitudinal component, v-transverse component and w-vertical component, respectively; and $\alpha_u = 0.5 \pm 0.05$ [54,55] and $\kappa = 0.4$ is von Kármán's constant;
- $f = nz/U(z)$ is the reduced frequency and $U(z) = U$ is the average horizontal wind speed;
- $\psi_\epsilon = \epsilon_b z_i / w_*^3$ is the dimensionless dissipation rate, $\epsilon_b = \Xi\left(w_*^3/z_i\right)$ is the average thermal dissipation rate of EKT [56–58]; to $\Xi = \left[\left(1 - \frac{z}{z_i}\right)^2 \left(\frac{z}{-L}\right)^{-2/3} + 0.75\right]^{3/2}$ [57] or $\Xi = 0.081 + 0.335 \exp\left[-\frac{\left(\frac{z}{z_i} - 0.2\right)}{0.588}\right]$ [59] and L is the length of Monin-Obukhov;
- $w_* = (u_*)_0 \left(z_i/(\kappa|L|)\right)^{1/3}$ is the convective velocity scale and $(u_*)_0$ is the surface friction velocity;
- $(f_m^*)_i = z/\left(\lambda_m\right)_i$ is the reduced frequency of the convective spectral peak, where $\left(\lambda_m\right)_i$ is the wavelength associated with the maximum of the vertical spectrum [25,60,61], with: $\left(\lambda_m\right)_u = \left(\lambda_m\right)_v = 1.5 z_i$ and $\left(\lambda_m\right)_w = 1.8\, z_i \left[1 - \exp\left(\frac{-4z}{z_i}\right) - 0.0003\, \exp\left(\frac{8z}{z_i}\right)\right]$;

For $k = 2\pi n/U$, the one-dimensional spectra are related by $F_i\left(k\right) = \frac{U}{2\pi} S_i^E\left(n\right)$, therefore

$$F_i\left(k\right) = \frac{a_i}{\left(1 + b_i k\right)^{\frac{5}{3}}},$$

for $a_i = \frac{1.06}{2\pi}\, c_i\, \psi_\epsilon^{2/3} \left(\frac{z}{z_i}\right)^{5/3} z_i {w_*}^2 \left[(f_m^*)_i\right]^{-5/3}$, $b_i = \frac{1.5}{2\pi} \left(\frac{z}{z_i}\right) z_i \left[(f_m^*)_i\right]^{-1}$ and $i = u, v, w$.

For a homogeneous turbulence situation in all directions, the three-dimensional spectrum for isotropic turbulence will depend only on the longitudinal spectrum F_u [3] and [4] (p. 30), given by:

$$k^3 \frac{d}{dk}\left(\frac{1}{k}\frac{dF_u}{dk}\right) = \frac{5a_u b_u k\,(3 + 11 b_u k)}{9\,(1 + b_u k)^{11/3}}.$$

The meteorological parameters calculated for the CBL are reported in Table A1.

Table A1. Meteorological parameters for CBL. Data obtained from experiment B of [51,62,63].

z_i	$(\overline{w\theta_0})$	$\frac{z_i}{L}$	Ω	u_*	u_g	v_g	ν	γ_c	$\frac{\partial\theta}{\partial z}$	f_c
1100	0.06	−18	7.27×10^{-5}	0.56	10	10	1.5×10^{-5}	10^{-3}	10^{-3}	10^{-4}

References

1. Hinze, J.O. *Turbulence*; Mc Graw Hill: New York, NY, USA, 1975; p. 790.
2. Tennekes, H.; Lumley, J.K. *A First Course in Turbulence*; The MIT Press: Cambridge, MA, USA, 1972; p. 301.
3. Kristensen, L.; Lenschow, D.; Kirkegaard, P.; Courtney, M. The spectral velocity tensor for homogeneous boundary-layer turbulence. *Bound.-Layer Meteorol.* **1989**, *47*, 149–193. [CrossRef]
4. Szinvelski, C.R.P. Uma Solução Para a Equação da Energia Cinética Turbulenta Empregando o Método das Características. Ph.D. Thesis, Universidade Federal de Santa Maria, Santa Maria, Brazil, 2009.
5. Goulart, A.G.O. Desenvolvimento de um Modelo Espectral para o Estudo do Decaimento da Turbulência na Camada Limite Convectiva. Ph.D. Thesis, Universidade Federal De Santa Maria-UFSM, Santa Maria, Brazil, 2001.
6. John, F. *Partial Differential Equations*, 2nd ed.; Sprienger-Verlag New York Inc.: New York, NY, USA, 1982; p. 259.
7. Iório, V.M. *EDP. Um Curso de Graduação*, 2nd ed.; IMPA: Rio de Janeiro, Brazil, 2001; p. 300.
8. Szinvelski, C.R.P.; Degrazia, G.A.; Goulart, A.G. Um modelo híbrido para evolução espectral da densidade de energia no período da manhã. *Ciência Natura*, **2009**, Edição Especial: VI Workshop Brasileiro de Micrometeorologia, 41–44. Available online: https://periodicos.ufsm.br/cienciaenatura/article/view/9512 (accessed on 20 September 2019)
9. Degrazia, G.A.; Rizza, U.; Mangia, C.; Tirabassi, T. Validation of a new turbulent parameterization for dispersion models in convective conditions. *Bound.-Layer Meteorol.* **1997**, *85*, 243–254. [CrossRef]
10. Folland, G.B. *Introduction to Partial Differential Equations*, 2nd ed.; Princeton Academic Press: Princeton, NJ, USA, 1995.
11. Degrazia, G.A.; Buligon, L.; Szinvelski, C.R.P.; Moor, L.; Costa Acevedo, O. Uma revisão teórica sobre funções de Autocorrelação aplicadas a altas e baixas Velocidades do vento. *Ciência Natura* **2014**, *36*. [CrossRef]
12. Taylor, G.I. Diffusion by continuous movements. *Proc. Lond. Math. Soc.* **1921**, *20*, 196–212.
13. Tennekes, A.H. The exponential Lagrangian correlation function and turbulent diffusion in the inertial subrange. *Atmos. Environ.* **1979**, *13*, 1565–1568. [CrossRef]
14. Batchelor, G.K. The Theory of Homogeneous Turbulence. *The Theory of Homogeneous Turbulence*; Cambridge University Press: Cambridge, UK, 1953.
15. Degrazia, G.A.; Anfonssi, D.; Campos Velho, H.F.; Ferrero, E. A Lagrangian decorrelation time scale fin the Convective Boundary Layer. *Bound.-Layer Meteorol.* **1998**, *86*, 525–534. [CrossRef]
16. Degrazia, G.A.; Anfonssi, D.; Carvalho, J.C.; Mangia, C.; Tirabassi, T.; Campos Velho, H.F. Turbulence parameterisation for PBL dispersion models in all stability conditions. *Atmos. Environ.* **2000**, *34*, 3575–3583. [CrossRef]
17. Degrazia, G.A.; Moreira, D.M.; Vilhena, M.T. Derivation of an eddy diffusity depending on source distance for vertically inhomogeneous turbulence in a convective boundary layer. *J. Appl. Meteorol.* **2001**, *40*, 1233–1240. [CrossRef]
18. Anfossi, D.; Oettl, D.; Degrazia, G.; Goulart, A. An analysis of sonic anemometer observations in low wind speed conditions. *Bound.-Layer Meteorol.* **2005**, *114*, 179–203. [CrossRef]
19. Phillips, P.; Panofsky, H. A re-examination of lateral dispersion from continuous sources. *Atmos. Environ.* **1982**, *16*, 1851–1859. [CrossRef]

20. Moor, L.; Degrazia, G.A.; Stefanello, M.B.; Mortarini, L.; Acevedo, O.C.; Maldaner, S.; Szinvelski, C.R.; Roberti, D.R.; Buligon, L.; Anfossi, D. Proposal of a new autocorrelation function in low wind speed conditions. *Phys. A Stat. Mech. Appl.* **2015**, *438*, 286–292. [CrossRef]
21. Manomaiphiboon, K.; Russell, A.G. Evaluation of some proposed forms of Lagrangian velocity correlation coefficient. *Int. J. Heat Fluid Flow* **2003**, *24*, 709–712. [CrossRef]
22. Szinvelski, C.R.; Buligon, L.; Stefanello, M.B.; Maldaner, S.; Roberti, D.R.; Degrazia, G.A. Testing Physical and Mathematical Criteria in a New Meandering Autocorrelation Function. In *Turbulence Modelling Approaches-Current State, Development Prospects, Applications*; IntechOpen: London, UK, 2017. [CrossRef]
23. Gardiner, C.W. *Handbook of Stochastic Methods for Physics, Chemistry and the Natural Sciences*; Springer: Berlin, Germany, 1985; p. 442.
24. Degrazia, G.A.; Goulart, A.G.O. Aplicações da Dinâmica de Fluidos em escoamentos na Camada Limite Planetária. *Ciência e Natura* **2005**, Edição Especial, 10–57. Available online: https://repositorio.ufsm.br/bitstream/handle/1/2652/Guerra_Thiago.pdf?sequence=1&isAllowed=y (accessed on 20 September 201).
25. Kaimal, J.C.; Wyngaard, D.A.; Haugen, D.A.; Coté, O.R.; Izumi, Y.; Caughey, S.J.; Readings, C.J. Turbulence structure in the Convective Boundary Layer. *J. Atmos. Sci.* **1976**, *33*, 2152–2226. [CrossRef]
26. Yeh, T.; Atta, C. Spectral transfer of scalar and velocity fields in heated-grid turbulence. *J. Fluid Mech.* **1973**, *58*, 233–261. [CrossRef]
27. Comte-Bellot, G.; Corrsin, S. The use of a contraction to improve the isotropy of grid-generated turbulence. *J. Fluid Mech.* **1966**, *25*, 657–682. [CrossRef]
28. Buligon, L.; Szinvelski, C.R.P. *Solução do Modelo de Pluma Gaussiana via Transformada de Fourier*, 1st ed.; Gráfica Editora Pallotti: Santa Maria, Brazil, 2010; p. 240.
29. Lumley, J.; Panofsky, H. *The Structure of Atmospheric Turbulence*; Interscience-Wiley: New York, NY, USA, 1964.
30. McComb, W. *The Physics of Fluid Turbulence*; Clarendon Press: Oxford, UK, 1992.
31. Kolmogorov, A.N. The local structure of turbulence in incompressible viscous fluid for large Reynolds number. *Dokl. Akad. Nauk SSSR* **1941**, *30*, 9–13. [CrossRef]
32. Medeiros, L.E. Decaimento da Turbulência na Camada Superficial. Ph.D. Thesis, Universidade Federal De Santa Maria—UFSM, Santa Maria, Brazil, 2005.
33. Stull, R.B. *An Introduction to Boundary Layer Meteorology*; Kluwer Academic Publishers: Dordrecht, The Netherlands, 1988; p. 666.
34. Pao, Y. Structure of Turbulent Velocity and Scalar Fields at Large Wavenumbers. *Phys. Fluids* **1965**, *8*, 1063–1075. [CrossRef]
35. Batchelor, G.K. Diffusion in a field of homogeneous turbulence, Eulerian analysis. *Aust. J. Sci. Res.* **1949**, *2*, 437–450. [CrossRef]
36. Abentroth, R.A. Parametrização do Decaimento da turbulência na Camada Limite Convectiva. Ph.D. Thesis, Universidade Federal Do Rio Grande do Sul—UFRGS, Porto Alegre, Brazil, 2007.
37. Nunes, A.B.; Campos Velho, H.F.; Satyamurty, P.; Degrazia, G.; Goulart, A.; Rizza, U. Morning Boundary-Layer Turbulent Kinetic Energy by Theoretical Models. *Bound.-Layer Meteorol.* **2009**, *134*, 23. [CrossRef]
38. Goulart, A.G.; Moreira, D.M.; Vilhena, M.T.; Degrazia, G.A.; Zilitinkevich, S.S. A New Model for the CBL Growth Based on the Turbulent Kinetic Energy Equation. *Environ. Fluid Mech.* **2007**, *007*, 409–419. [CrossRef]
39. Goulart, A.; Degrazia, G.A.; Rizza, U.; Anfossi, D. A Theorical Model for the Study of Convective Turbulence Decay and Comparison with Large-Eddy Simulation Data. *Bound. Layer-Meteorol.* **2003**, *107*, 143–155. [CrossRef]
40. Sorbjan, Z. Decay of convective turbulence revisited. *Bound.-Layer Meteorol.* **1997**, *82*, 501–515. [CrossRef]
41. Goulart, A.G.; de Vilhena, M.T.M.B.; Moreira, D.M.; Bodman, B.E.J. An Analytical Solution for the Nonlinear Spectrum Equation by the Decomposition Method. *J. Phys. A* **2008**, *41*, 8. [CrossRef]
42. Degrazia, G.; Goulart, A.; Anfossi, D.; Campos Velho, H.; Lukaszcyk, P.; Palandi, J. A model based on Heisenberg's theory for the eddy diffusivity in decaying turbulence applied to the residual layer. *Nuovo Cimento-Soc. Ital. Fisica Sez. C* **2003**, *26*, 39–52.
43. Teschl, G. *Ordinary Differential Equations and Dynamical Systems*; American Mathematical Soc.: Providence, RI, USA, 2010; Volume 140.
44. Doering, C.I.; Lopes, A.O. *Equações Diferencias Ordinárias*, 1st ed.; IMPA: Rio de Janeiro, Brazil, 2005; p. 421.

45. Biezuner, R.J. *Notas de Aula: Equações Diferenciais Parciais I/II*. 2010. Disponível em. Available online: http://arquivoescolar.org/bitstream/arquivo-e/151/1/edp.pdf (accessed on 8 October 2019).
46. Alonso, I.P. *Primer Curso de Ecuaciones en Derivadas Parciales*. Almeria, ES, 2005; p. 334. Available online: http://matematicas.uam.es/~ireneo.peral/libro.pdf (accessed on 8 October 2019).
47. Evans, L.C. *Partial Diferential Equations—Graduate Studies in Mathematics—Volume 19*, 2nd ed.; Americam Mathematical Society: Providence, RI, USA, 2010; p. 662.
48. Buligon, L.; Degrazia, G.; Szinvelski, C.; Goulart, A. Algebraic Formulation for the Dispersion Parameters in an Unstable Planetary Boundary Layer: Application in the Air Pollution Gaussian Model. *Open Atmos. Sci. J.* **2008**, *2*, 153–159. [CrossRef]
49. Goulart, A.G.; Vilhena, M.T.; Degrazia, G.A.; Flores, D.T. Vertical, lateral and longitudinal eddy diffusivities for a decaying turbulence in the convective boundary layer. *Ecol. Model.* **2007**, *204*, 516–522. [CrossRef]
50. Goulart, A.G.; Degrazia, G.A.; Campos, C.; Silveira, C.P. Coeficientes de difusão turbulentos para a camada residual. *Rev. Bras. De Meteorol.* **2004**, *19*, 123–128.
51. Moeng, C.; Sullivan, P. Evaluation of Turbulent Transport and Dissipation Closures in Second-Order Modeling. *J. Atmos. Sci.* **1989**, *46*, 2311–2330. [CrossRef]
52. Levandosky, J. *Math 220A. Partial Differential Equations of Applied Mathematics*. Stanford, CA, USA, 2002. Disponível em. Available online: http://www.stanford.edu/class/math220a/handouts/firstorder.pdf (accessed on 8 October 2019).
53. Lima, E.L. *Curso de Análise Volume 2*, 6th ed.; Instituto de Matemática Pura e Aplicada: Rio de Janeiro, Brazil, 2000; p. 557.
54. Champagne, F.H.; Friehe, C.A.; Larve, J.C.; Wyngaard, J.C. Flux measurements, flux estimation techniques, and fine scale turbulence measurements in the instable surface layer over land. *J. Atmos. Soc.* **1977**, *34*, 515–520. [CrossRef]
55. Sorbjan, Z. *Structure of the Atmospheric Boundary Layer*; Prentice Hall: Englewood Cliffs, NJ, USA, 1989; p. 317.
56. Caughey, S.J.; Palmer, S.G. Some aspects of turbulence structure through the depth of the convective boundary layer. *Q. J. R. Meteorol. Soc.* **1979**, *105*, 811–827. [CrossRef]
57. Hϕjstrup, J. Velocty spectra in the unstable surface planetary boundary layer. *J. Atmos. Sci.* **1982**, *39*, 2239–2248.
58. Wilson, K. A three-dimensional correlation/spectral model for turbulent velocities in a convective boundary layer. *Bound.-Layer Meteorol.* **1997**, *85*, 35–52. [CrossRef]
59. Moeng, C. A large-eddy-simulation model for the study of planetary boundary-layer turbulence. *J. Atmos. Sci.* **1984**, *41*, 2052–2062. [CrossRef]
60. Caughey, S.J. Observed Characteristics of the Atmospheric Boundary Layer. In *Atmospheric Turbulence and Air Pollution Modelling*; Nieuwstdat, F.T.M., van Dop, H., Eds.; Springer: Dordrecht, The Netherlands, 1982; pp. 107–158. [CrossRef]
61. Degrazia, G.A.; Anfonssi, D. Estimation of the Kolmogorov constant C_0 from classical statistical diffusion theory. *Atmos. Environ.* **1998**, *32*, 3611–3614. [CrossRef]
62. Moeng, C.; Sullivan, P. A comparison of shear-and buoyancy-driven planetary boundary layer flows. *J. Atmos. Sci.* **1994**, *51*, 999–1022. [CrossRef]
63. Nieuwstadt, F.; Brost, R. The Decay of Convective Turbulence. *J. Atmos. Sci.* **1986**, *43*, 532–546. [CrossRef]